

**NIST GCR 99-782**

---

---

**FLAME SPREAD MODEL PROGRESS:  
ENHANCEMENTS AND USER INTERFACE**

---

---

**Michael J. Spearpoint, and  
Scott E. Dillon**

**NIST**

**United States Department of Commerce  
Technology Administration  
National Institute of Standards and Technology**

**NIST GCR 99-782**

---

---

**FLAME SPREAD MODEL PROGRESS:  
ENHANCEMENTS AND USER INTERFACE**

---

**Prepared for**

**U.S. Department of Commerce  
Building and Fire Research Laboratory  
National Institute of Standards and Technology  
Gaithersburg, MD 20899**

**By**

**Michael J. Spearpoint  
University of Maryland  
College Park, MD 20742  
and  
Scott E. Dillon  
Southwest Research Institute  
San Antonio, TX 78238**

**October 1999**

**Issued November 1999**



## Notice

**This report was prepared for the Building and Fire Research Laboratory of the National Institute of Standards and Technology under Contract number 60NANB6D0120. The statement and conclusions contained in this report are those of the authors and do not necessarily reflect the views of the National Institute of Standards and Technology or the Building and Fire Research Laboratory.**

**FLAME SPREAD MODEL PROGRESS : ENHANCEMENTS & USER  
INTERFACE**

Michael Spearpoint  
Department of Fire Protection Engineering  
University of Maryland  
College Park, MD 20742

Scott E. Dillon  
Department of Fire Technology  
Southwest Research Institute  
San Antonio, TX 78238

October 1999

Prepared for:

U.S. Department of Commerce  
National Institute of Standards and Technology  
Laboratory of Building and Fire Research  
Washington, D.C. 20234

## **Flame spread model progress : Enhancements & user interface**

M. J. Spearpoint and S. E. Dillon

### **ABSTRACT**

This report describes the enhancements made to Quintiere's flame spread model based on worked published in the literature by other researchers. The height of the ignition source flame, its extension under a horizontal ceiling and the incident heat flux to a target material have been addressed.

The results from the enhanced version of the model have been compared with those obtained from an earlier version of the model and with experimental data. The new version generally shows an improvement over the previous versions although there are isolated instances in which this is not the case.

This report also briefly describes a user-friendly windows based front-end that has been developed for the enhanced version of the model. The interface can be used to read in existing model input files, create new input files, execute the main QFSM program and create simple on screen plots of the results. The front-end also includes an online help file that describes the various input parameters. A single self-extracting file containing the QFSM model, the interface, the help documentation and associated support files has been created to simplify distribution and installation of the software.

Keywords: computer model, corner test, fire growth, flame spread

## TABLE OF CONTENTS

<b>1. BACKGROUND</b> .....	<b>1</b>
<u>1.1 Flame spread model</u> .....	1
<u>1.2 The ISO 9705 room/corner test</u> .....	2
<b>2. MODEL ENHANCEMENTS</b> .....	<b>3</b>
<u>2.1 Vertical flame height</u> .....	3
<u>2.2 Flame length under a ceiling</u> .....	10
<u>2.3 Initial ignition height</u> .....	14
<u>2.4 Burner heat flux</u> .....	15
<u>2.5 Flame spread heat flux</u> .....	18
<u>2.6 Summary of current QFSM relationships</u> .....	18
<b>3. COMPARISON WITH PREVIOUS DATA</b> .....	<b>19</b>
<u>3.1 Times to flashover</u> .....	19
<u>3.2 Performance ranking</u> .....	25
<u>3.3 Energy release</u> .....	26
<b>4. USER INTERFACE</b> .....	<b>36</b>
<b>5. CONCLUSIONS</b> .....	<b>38</b>
<b>6. REFERENCES</b> .....	<b>39</b>

## LIST OF TABLES

<u>Table 1. Comparison times to flashover from experimental test data and QFSM predictions using properties given by Quintiere <i>et al.</i> [5].</u>	21
<u>Table 2. Comparison times to flashover from experimental test data and QFSM predictions using properties given by Quintiere <i>et al.</i> [24].</u>	24
<u>Table 3. Comparison times to flashover from full-scale test results and QFSM predictions for FAA data.</u>	25

## LIST OF FIGURES

<u>Figure 1. Features of Quintiere's fire growth model.</u>	1
<u>Figure 2. Schematic of the ISO 9705 room/corner test.</u>	3
<u>Figure 3. Dependence of incident heat flux on dimensionless flame height above burner surface.</u>	6
<u>Figure 4. Burner flame lengths in a corner and under a ceiling.</u>	8
<u>Figure 5. Flame height against energy release relationships and observations for <math>D = 0.17</math> m except where indicated.</u>	9
<u>Figure 6. Comparison Andersson &amp; Giacomelli [15] data, Thomas &amp; Karlsson [13] correlation and Babrauskas [14] correlations for a ceiling height of 0.40 m.</u>	11
<u>Figure 7. Comparison Andersson &amp; Giacomelli [15] data, Thomas &amp; Karlsson [13] correlation and Babrauskas [14] correlations for a ceiling height of 0.73 m.</u>	12
<u>Figure 8. Comparison between flame extension lengths for the ISO 9705 room/corner configuration.</u>	13
<u>Figure 9. Transition from corner flame to flame extension under a ceiling.</u>	14
<u>Figure 10. Heat flux from a burner flame as a function of dimensionless flame height.</u>	16
<u>Figure 11. Maximum heat flux as a function of burner dimension.</u>	17
<u>Figure 12. Sensitivity of predicted energy release rate by QFSM v1.4 for Test E6, FR Particle Board Type B1.</u>	22
<u>Figure 13. Comparison of the predicted energy release rate by QFSM for Test E7, Combustible Faced Mineral Wool.</u>	23

<u>Figure 14. Comparison between the experimental data and the predicted times to flashover from QFSM v1.3.</u> .....	24
<u>Figure 15. Comparison between the experimental data and the predicted times to flashover from QFSM v1.4.</u> .....	25
<u>Figure 16. Comparison between measured and predicted energy release, LSF Test R 4.01, Fire retarded chipboard.</u> .....	26
<u>Figure 17. Comparison between measured and predicted energy release, LSF Test R 4.02, Paper faced gypsum board.</u> .....	27
<u>Figure 18. Comparison between measured and predicted energy release, LSF Test R 4.04, Polyurethane panel with paper facing.</u> .....	28
<u>Figure 19. Comparison between measured and predicted energy release, LSF Test R 4.05, Extruded polystyrene board.</u> .....	29
<u>Figure 20. Comparison between measured and predicted energy release, LSF Test R 4.06, Acrylic glazing.</u> .....	30
<u>Figure 21. Comparison between measured and predicted energy release, LSF Test R 4.07, Fire retarded PVC.</u> .....	30
<u>Figure 22. Comparison between measured and predicted energy release, LSF Test R 4.08, 3-layered fire retarded polycarbonate panel.</u> .....	31
<u>Figure 23. Comparison between measured and predicted energy release, LSF Test R 4.09, Varnished massive timber.</u> .....	32
<u>Figure 24. Comparison between measured and predicted energy release, LSF Test R 4.10, Fire retarded plywood.</u> .....	33
<u>Figure 25. Comparison between measured and predicted energy release, LSF Test R 4.11, Normal plywood.</u> .....	33
<u>Figure 26. Comparison between measured and predicted energy release, LSF Test R 4.20, Fire retarded expanded polystyrene board (40 mm).</u> .....	34
<u>Figure 27. Comparison between measured and predicted energy release, LSF Test R 4.21, Fire retarded expanded polystyrene board (80 mm).</u> .....	35
<u>Figure 28. The QFSM interface data input window.</u> .....	37
<u>Figure 29. The QFSM interface output analysis window.</u> .....	38

## NOMENCLATURE

$A$	Area [ $\text{m}^2$ ]
$C$	Hasemi's flame height constant [-]
$D$	burner width [m]
$\varepsilon$	emissivity [-]
$H$	height [m]
$H^*$	virtual height [m]
$\kappa$	absorption coefficient [ $\text{m}^{-1}$ ]
$l_m$	mean beam length [m]
$L$	length [m]
$\dot{Q}$	energy release rate [kW]
$Q^*$	dimensionless energy release rate [-]
$\dot{q}''$	heat flux per unit area [ $\text{kW}/\text{m}^2$ ]
$g$	gravitational acceleration [ $9.81 \text{ m}/\text{s}^2$ ]
$k_f$	Quintiere's flame length coefficient [ $0.067 (\text{m}^5/\text{kW}^2)^{1/3}$ or approximately $0.01 \text{ m}^2/\text{kW}$ ]
$c_p$	specific heat capacity [ $\text{J}/\text{kg}\cdot\text{K}$ ]
$\rho$	density [ $\text{kg}/\text{m}^3$ ]
$\sigma$	Stefan-Boltzmann constant [ $\text{W}/\text{m}^2\cdot\text{K}$ ]
$T$	temperature [ $^{\circ}\text{C}$ or $\text{K}$ ]
$V$	volume [ $\text{m}^3$ ]
$x, y, z$	coordinates [m]

### Subscripts

$0$	initial, ambient
$f$	flame
$i$	incident
$ig$	ignition source
$p$	pyrolysis
$b$	burn-out
$n$	flame length power [2/3 or approximately 1]

### Superscripts

$( )''$	per unit area
$( )'$	per unit length
$( \dot{ } )$	per unit time

# Flame spread model progress : Enhancements & user interface

M. J. Spearpoint and S. E. Dillon

## 1. BACKGROUND

### 1.1 Flame spread model

Quintiere's flame spread (or fire growth) model computes the wind-aided (upward and ceiling jet) and opposed flow (lateral and downward) flame spread front as well as the associated burn-out fronts for a material lining the walls and ceiling of a compartment. The pyrolysis and burn-out fronts are then used to compute the total burning area as shown in Figure 1. The model also predicts the upper gas layer temperature and the rate of energy release as a function of time. Enhanced flame spread due to thermal feedback effects from the room are included however oxygen depletion is not. Previous literature has been published which describes the physics of the model and its application [1], [2], [3], [4], [5] in more detail.

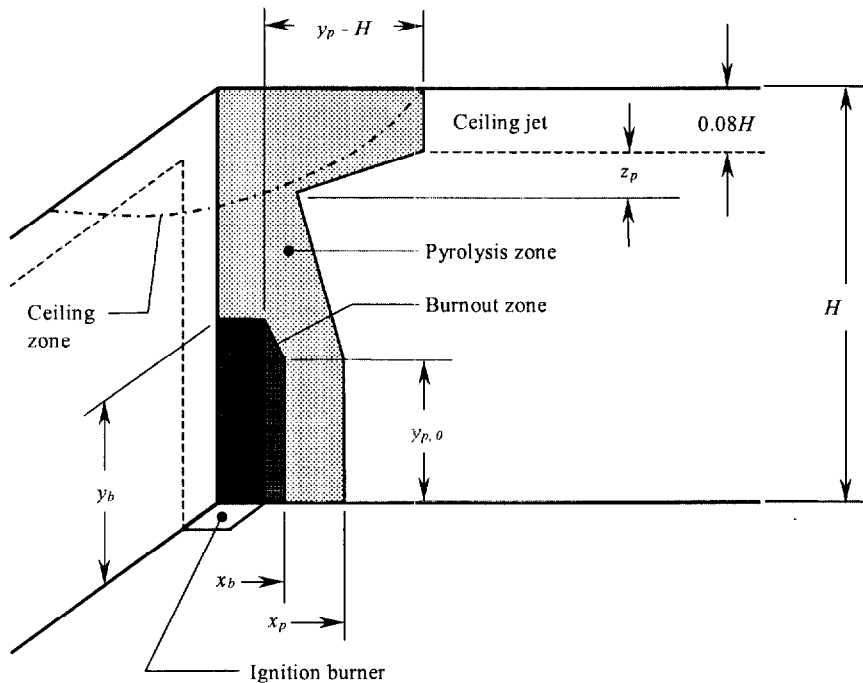


Figure 1. Features of Quintiere's fire growth model.

In developing the model, Quintiere necessarily had to make several estimations regarding the characteristics of the burner flame. These estimates are addressed in more detail in subsequent sections of this report. However, since the initial development of the model, work on the flame characteristics in various wall/ceiling configurations have been published by several researchers. These data are relevant to making enhancements to QFSM and remove some of the estimates made by Quintiere for certain parameters where no information was available at the time. This study begins to make these enhancements and suggest where further work is applicable.

The original QFSM code was written in FORTRAN and has subsequently been modified by Dillon [6]. More recent additions have been made for this report, the previous version of QFSM last modified by Dillon is referred to as v1.3 and the new version developed for this study is referred to as v1.4.

Previous versions of QFSM have run under a command-line driven DOS environment. With the advent of Windows based operating systems there is the ability and expectation have a more user-friendly interface to any program. This report also details a new graphical front-end to QFSM that does not sacrifice the ability for the main code to be run under a command-line driven DOS environment.

## **1.2 The ISO 9705 room/corner test**

The ISO 9705 Full-Scale Room Fire Test for Surface Products [7] (or more simply the room/corner test) has the following criteria and a schematic of the test compartment is shown in Figure 2:

- Room: 2.4 m x 3.6 m x 2.4 m high.
- Door on short wall: 2.0 m x 0.8 m wide.
- Ignition burner: 17 cm x 17 cm square sand burner, top surface  
30 cm above the floor, propane fuel.
- Burner location: Corner, in contact with both walls.
- Burner output: 100 kW for 10 minutes followed by 300 kW for an  
additional 10 minutes.

- Material mounting: On the 3 walls opposite the doorway and on the ceiling if desired.

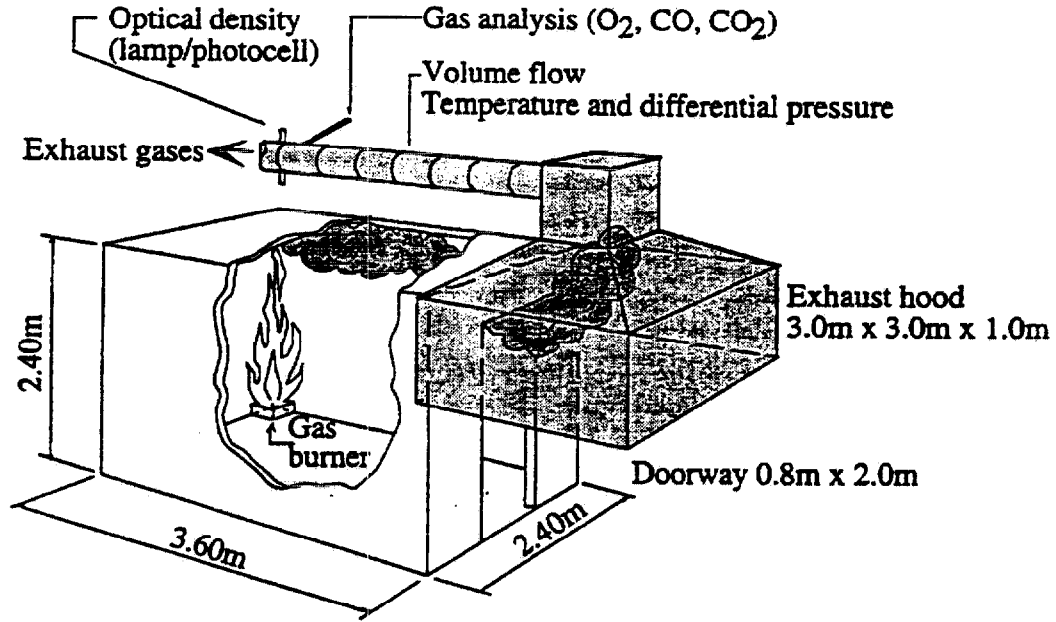


**Figure 2.** Schematic of the ISO 9705 room/corner test.

## 2. MODEL ENHANCEMENTS

### 2.1 Vertical flame height

Flame height can be defined in several different ways such as the height of the continuous region, the height of the flame tips or some ‘average’ height. These alternative definitions can complicate comparisons between various measurements and correlations.

In the previous version of QFSM the ‘average’ vertical height for the flame was assumed by Quintiere [1] to follow a correlation for an equivalent line-source such that

$$y_f = y_b + k_f \left[ \dot{Q}'_{ig} + \dot{Q}''(y_p - y_b) \right]^n, \quad y_b \leq k_f \dot{Q}'_{ig} \quad (1)$$

and

$$y_f = y_b + k_f \left[ \dot{Q}''(y_p - y_b) \right]^n, \quad y_b \geq k_f \dot{Q}'_{ig} \quad (2)$$

with:  $k_f = 0.067 \text{ (m}^5/\text{kW}^2)^{1/3}$  or approximately  $0.01 \text{ m}^2/\text{kW}$   
and  $n = 2/3$  or approximately 1.

Since the publication of Quintiere's work, several researchers have considered the height of flames of a fire in a corner and of particular interest here is to consider the flame height for the propane burner used in the standard ISO 9705 room/corner test. It is necessary to know the height of the flame so that appropriate values can be input into QFSM.

### Kokkala

The work by Kokkala [8] shows methods for determining this flame height. This method will be used to determine the flame height for the 100 kW, 300 kW and eventually a 900 kW fire. Although the standard ISO 9705 room test only requires energy release rates of 100 kW and 300 kW, work has been done as a part of the EUREFIC program in Europe to evaluate the performance of materials exposed to larger fires in larger compartments [9].

From Kokkala's work, a flame height can be calculated based on the energy release rate of the burner. The ratio of the flame height over the burner dimension  $H_f/D$  is a function of the rate of energy release from the burner. To determine the flame height, a dimensionless energy release rate  $Q^*$  must be determined based on work by Zukoski [10]:

$$Q^* = \frac{\dot{Q}}{\rho_0 c_{p,0} T_0 g^{1/2} D^{5/2}} \quad (3)$$

with:  $\dot{Q}$  = energy release of the burner in kW

D = the burner dimension (diameter or width) in m

$T_0 = 300 \text{ K}$

$\rho_0 = 1.1614 \text{ kg/m}^3$

$c_{p,0} = 1.007 \text{ kJ/kg}\cdot\text{K}$

$g = 9.81 \text{ m/s}^2$

which results in:

$$Q^* = \frac{\dot{Q}}{1099D^{5/2}}. \quad (4)$$

This is comparable to the work by Gross [11], in which the ambient fluid properties he uses results in a value of 1116 in the denominator.

Based on Equation (3), dimensionless energy release rates can be calculated for 100 kW, 300 kW and 900 kW burner output levels such that:

$$Q^*_{100} = 7.6 \quad Q^*_{300} = 22.9 \quad Q^*_{900} = 68.7$$

Kokkala also reports that based on the  $Q^*$  value, a ratio between the average flame height  $H_f$  and the burner size  $D$  can be determined:

For  $Q^* < 8.6$ :

$$\frac{H_f}{D} = -1.73 + 4.96(Q^*)^{2/3}, \quad (5)$$

and for  $Q^* > 8.6$ :

$$\frac{H_f}{D} = 15.6 + 0.40Q^*. \quad (6)$$

Therefore, the average flame heights for the 0.17 m square burner located in the corner, with the above mentioned energy release rates are:

$$(H_f)_{100} = 3.0 \text{ m} \quad (H_f)_{300} = 4.2 \text{ m} \quad (H_f)_{900} = 7.3 \text{ m}$$

Due to the need for simplifying the heat flux from a complex and turbulent flame, the average flame heights calculated above can be revised by assuming that the heat flux is a constant value over the height of the flame. Kokkala's work shows that the heat flux incident to the walls of the corner is dependent on the dimensionless height above the burner  $y/H_f$  in accordance with the log-log graph that is shown in Figure 3. The data

shown in this graph was obtained using a square burner with heat output in the range of 40 kW to 300 kW and the graph presented here was created by extrapolating points off of a best-fit line through the data points for a 0.17 m square burner provided by Kokkala.

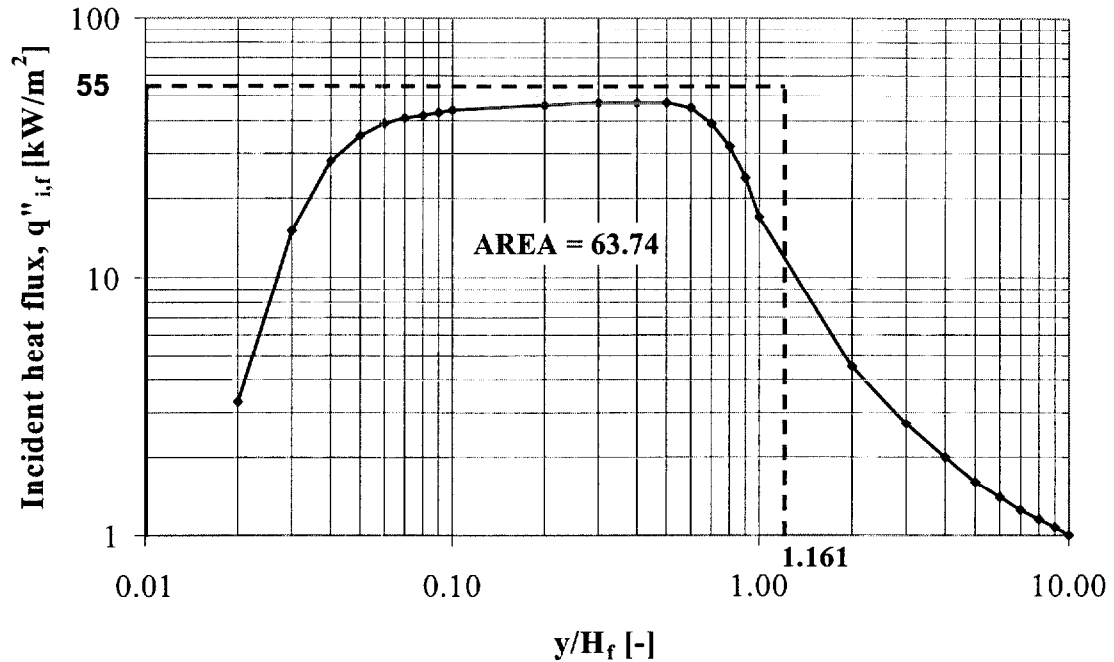


**Figure 3.** Dependence of incident heat flux on dimensionless flame height above burner surface.

Taking the maximum heat flux for a flame from Kokkala’s data as 55 kW/m<sup>2</sup>, and the area under the curve, an effective flame height for a constant heat flux can be determined. The area under this curve (63.74) was determined using the Trapezoidal Rule. A degree of error does exist in this calculation of the area due to the problems associated with extrapolating points from a log-log graph. However, it is believed that these errors are minimal.

Using the concept of a constant heat flux of 55 kW/m<sup>2</sup> over the height of the flame produces the rectangular curve shown in Figure 3. When identical area values are used, the following dimensionless flame height can be predicted:

$$y/H_f = 1.161 \quad (7)$$

This means that using the flame height results from above, a constant 55 kW/m<sup>2</sup> heat flux will be imposed by flame heights of:

$$(H_f)_{100} = 3.5 \text{ m} \quad (H_f)_{300} = 4.9 \text{ m} \quad (H_f)_{900} = 8.5 \text{ m}$$

### Hasemi

Hasemi [12] also performed analysis into the flame heights of corner burners. His analysis produces the following equation:

$$\frac{H_f}{D} = CQ^{*2/3} \quad (8)$$

with:  $C = 4.3$  for the flame tips

$C = 3.0$  for the continuous flame region

The continuous flame height is of significant importance due to the heat flux from the flames being the most intense and almost constant over this region. Thus, a value of  $C = 3.0$  was used and produced the following flame heights:

$$(H_f)_{100} = 2.0 \text{ m} \quad (H_f)_{300} = 4.1 \text{ m} \quad (H_f)_{900} = 8.6 \text{ m}$$

There are some potential limitations to using Hasemi's analysis to evaluate the flame heights at high burner heat outputs. The tests that Hasemi conducted in the formation of this correlation were for relatively low heat output levels compared with those used in the room/corner test.

### Visual

Full-scale ISO 9705 tests performed at the LSF laboratory in Italy for 12 different materials were used to determine the flame heights by visual observations. Analysis of the videotapes from these tests reveal much lower values for the flame heights for both the 100 kW and 300 kW fires than predicted by Kokkala's and Hasemi's equations.

Using a ruler and a marker an appropriate scale was drawn directly onto the screen of a

television set. The test for gypsum wallboard was then viewed at both regular and frame-by-frame speeds to determine the height of the region of continuous flame and the height of the flame tips. The gypsum wallboard test was chosen due to the lack of ignition and the low smoke production.

To determine the continuous flame region the tape was viewed frame-by-frame to determine at what height there was flame for approximately 95% of the time. Due to turbulence factors, a 100% assumption would have shown very low flame heights. This method revealed the following continuous flame heights:

$$(H_f)_{100} = 1.5 \text{ m} \quad (H_f)_{300} = 2.7 \text{ m}$$

It must be realized that for the 300 kW fire this dimension represents a distance from the top of the burner to the ceiling corner, 2.1 m, and then 0.6 m along the wall-ceiling interface (Figure 4) i.e.  $H_f = H + L_f$ . If the burner was placed in a space with a greater ceiling height it cannot readily be assumed that the observed flame height would be 2.7 m.

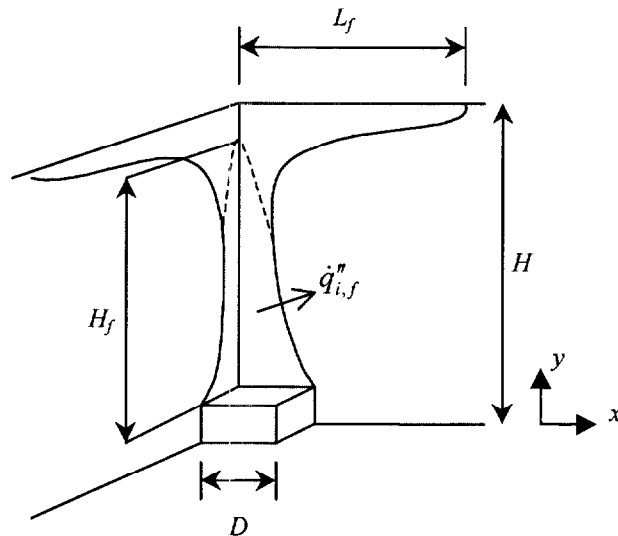


**Figure 4.** Burner flame lengths in a corner and under a ceiling.

In order to determine the overall height of the flame, 51 instantaneous, frame-by-frame measurements were taken for the 100 kW fire. The 300 kW fire was too large for accurate measurements to be taken given the camera angle—the flame tips were completely out of view. For the 100 kW fire a maximum flame tip height of 3.1 m and a minimum height of 2.1 m were recorded. The average of all of the recorded data yields an overall flame height of approximately 2.6 m.

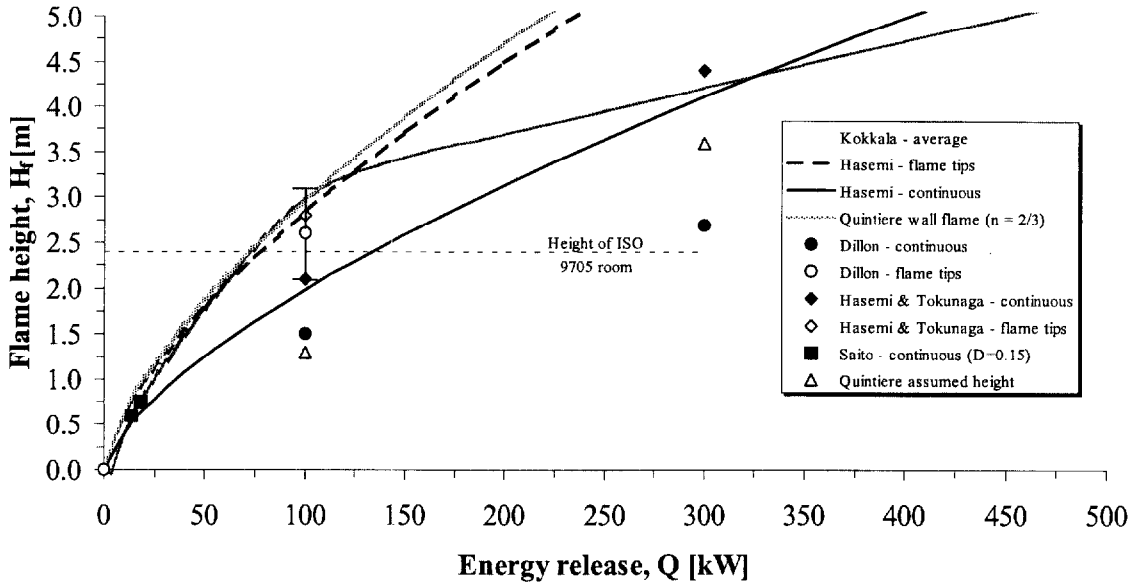


**Figure 5.** Flame height against energy release relationships and observations for  $D = 0.17$  m except where indicated.

Figure 5 shows the predicted flame lengths using either Kokkala's or Hasemi's relationships plus the flame length relationship originally suggested by Quintiere given by Equation (1) for a burner of width 0.17 m such that  $\dot{Q}' = \dot{Q} / D$ . In actuality, Quintiere *et al.* [5] use an estimated  $\dot{Q}'$  to obtain selected flame heights of

$$(H_f)_{100} = 1.3 \text{ m} \quad (H_f)_{300} = 3.6 \text{ m}.$$

In addition, Figure 5 shows the observed flame lengths at several energy release rates for the same size burner except in the case of Saito's data in which the burner the slightly smaller width of 0.15 m. It is clear that for flame heights below the ceiling

height of the ISO 9705 room the relationships given by Kokkala, Hasemi (flame tips) and Quintiere are almost exactly the same. Comparing the observed flame heights with the correlations, Dillon's observations are lower than the predicted values and also lower than those observations made by Hasemi & Tokunga.

It is also apparent that the correlations suggested by Kokkala and Hasemi diverge at higher energy release rates although in the case of the ISO 9705 room this is not relevant.

For the new version of QFSM, the vertical flame height correlation suggested by Hasemi for continuous flames, with  $\dot{Q} = \dot{Q}_{ig} + \dot{Q}_p'' \cdot A_p$ , has been selected as the most appropriate since it gives the closest match with Dillon's observations.

## 2.2 Flame length under a ceiling

Once the flame impinges on a horizontal ceiling the vertical flame height correlations no longer apply. Instead, we need to consider how a flame will extend horizontally under that ceiling. Thomas & Karlsson [13] and Babrauskas [14] both provide relationships for calculating this flame extension. The analysis and data used in each case were different and in this study the applicability of both for inclusion into QFSM are investigated.

Thomas & Karlsson [13] base their correlation for the flame extension due to a burner in a corner on the experimental data reported by Andersson & Giacomelli [15] and also the work by Gross [11]. In this case, the flame extension is defined as the distance between the corner vertex and the end of the continuous flame region. They obtain a relationship such that

$$\frac{L_f}{H^*} = -0.15 + 25Q^* \quad (9)$$

where

$$H^* = H + 3D \quad (10)$$

Babrauskas [14] considers flame extension lengths under unbounded and bounded ceilings with the plume either unrestricted or with its entrainment restricted by neighboring walls. The data Babrauskas uses to verify his correlation was published by You and Faeth [16] and it should be noted that the maximum energy release was only around 8 kW in those tests. This value is significantly less than the 100 kW and 300 kW burner fires employed in the ISO 9705 room/corner test.

Figure 6 and Figure 7 compare the data quoted by Andersson & Giacomelli [15] and used by Thomas & Karlsson [13] for their correlation with those correlations given by Babrauskas [14]. The maximum rate of energy release of the burner used in the experiments is less than the 100 kW minimum burner energy release required in the ISO 9705 room/corner test. For a ceiling height of 0.40 m, Babrauskas' 1/4 plume and 1/4 ceiling correlation does not compare well with Andersson & Giacomelli's data (shown as 'Sw.H - 0.40' in Figure 6). For the 0.73 m ceiling the match between Andersson & Giacomelli's data (shown as 'Sw.H - 0.73' in Figure 7) and Babrauskas' 1/4 plume and 1/4 ceiling correlation is reasonable for energy releases of 10 kW to around 30 kW.

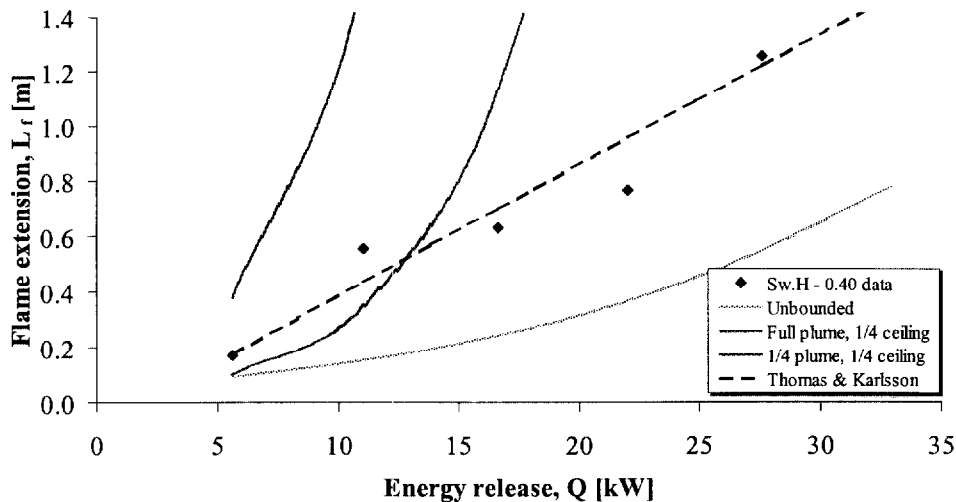


**Figure 6.** Comparison Andersson & Giacomelli [15] data, Thomas & Karlsson [13] correlation and Babrauskas [14] correlations for a ceiling height of 0.40 m.

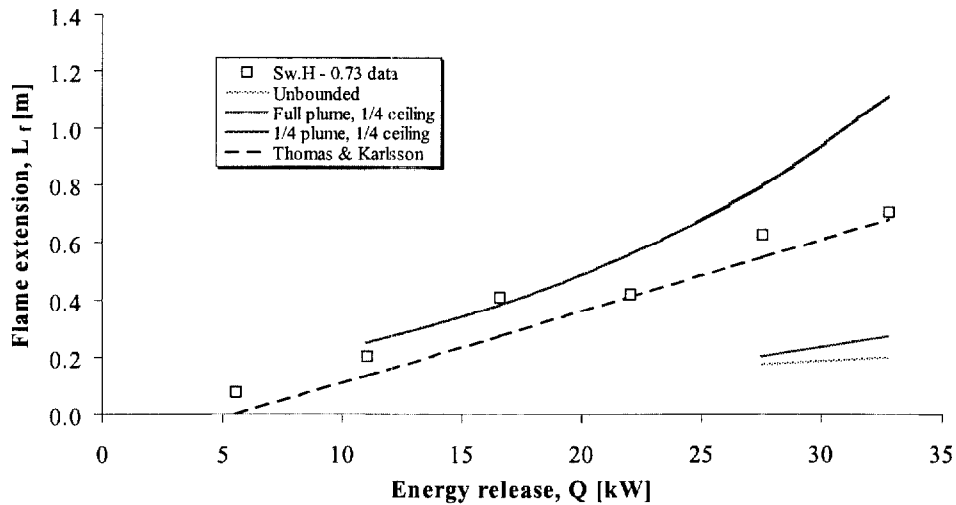


**Figure 7.** Comparison Andersson & Giacomelli [15] data, Thomas & Karlsson [13] correlation and Babrauskas [14] correlations for a ceiling height of 0.73 m.

Figure 8 shows the expected flame extension lengths for the ISO 9705 room/corner configuration with  $D = 0.17$  and  $H = (2.40 - 0.30) = 2.1$  m since, as noted in §1.2, the top surface of the burner is 0.30 m above the floor. For the ISO 9705 room, the bounded ceiling and restricted plume case would be the most appropriate of Babrauskas' correlations to consider. Flame extensions above 2.40 m are probably meaningless for the ISO 9705 room since this is the width of the compartment.

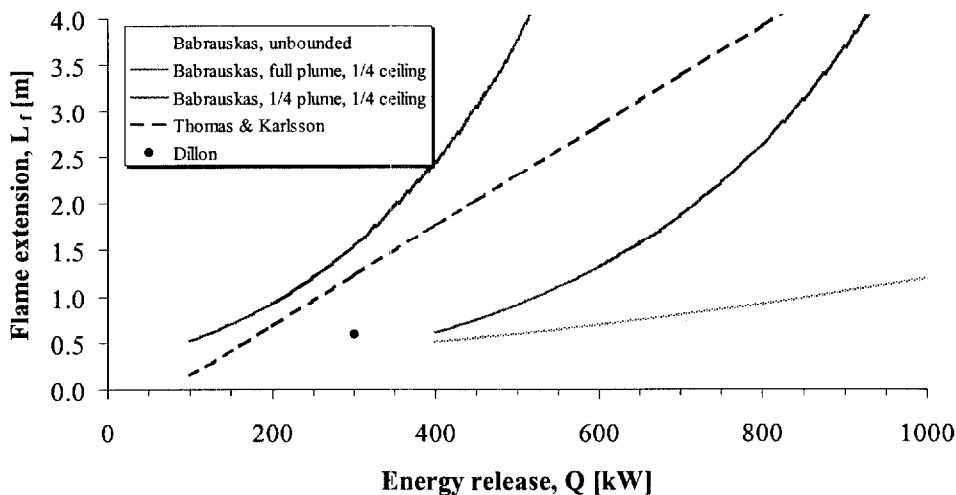


**Figure 8.** Comparison between flame extension lengths for the ISO 9705 room/corner configuration.

At energy release rates between around 150 kW and 300 kW the Thomas & Karlsson and Babrauskas 1/4 plume, 1/4 ceiling correlations for flame extension are similar. However, outside of that range, the correlations diverge significantly. Figure 8 also shows the measured flame extension length obtained by Dillon [17] for the 300 kW burner. The observed value is considerably less than those predicted by either Thomas & Karlsson or Babrauskas.

The Thomas & Karlsson prediction for flame extension at 300 kW is closer to Dillon's observed value and for the 100 kW burner Dillon did not observe any flame extension across the ceiling, which suggests from Figure 8 that the Thomas & Karlsson correlation is a better prediction for flame extension than given by Babrauskas. Thus, for the new version of QFSM the Thomas & Karlsson correlation given by Equation (9), has been included in the model whilst the burner and wall flames are contiguous. Once the wall flame breaks away from the burner flame, QFSM reverts to the calculation for flame length used in the previous version given by Equation (2).

It should be noted that the transition from Hasemi's flame height correlation to the Thomas & Karlsson flame extension is not continuous. Rather a step function in the

flame length occurs (Figure 9) when the rate of energy release goes from  $\dot{Q}_-$ , a rate of energy release such that  $H_f \leq H$  using Hasemi's correlation to  $\dot{Q}_+$  a rate of energy release such that  $H_f > H$  from Hasemi's correlation.

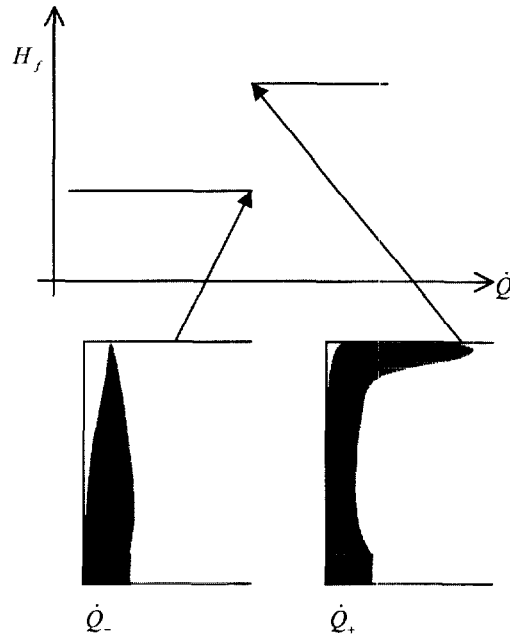


**Figure 9.** Transition from corner flame to flame extension under a ceiling.

### 2.3 Initial ignition height

In reality the ignition of a wall sample subjected to a vertical flame is unlikely to occur instantaneously over the whole surface under attack, any value used for the initial ignition height should account for this.

In the previous version of QFSM, the user supplied a value for the height of the initial ignition region  $y_{p,0}$ . For an ISO 9705 simulation this value was typically 1.3 m. This assumed value is less than the expected flame height from either the 100 kW or 300 kW burner.

Thus, the new version of QFSM assumes that the initial ignition height is that of the continuous flame length calculated from the Hasemi flame height and Thomas & Karlsson flame extension equations described above.

#### **2.4 Burner heat flux**

In the previous version of QFSM the heat flux from the burner flame was estimated to be  $60 \text{ kW/m}^2$  regardless of any variation in the burner size or energy release. In order to justify or modify this value, data from the literature was obtained and analyzed. Figure 10 shows the measured heat flux from burners flames with a range of  $D$  dimensions against dimensionless flame heights taken from several sources [8], [9], [17], [18], [19], [20], [21]. Data is shown for different  $x/D$  values depending on the source of the data. It is appreciated that Figure 10 is difficult to interpret with so many data presented on one chart. However, subject to a fair degree of scatter, the data suggests that the maximum incident flux is function of the burner size  $D$ .

Dillon's data was taken from corner tests with a ceiling and it can be seen in Figure 10 that the incident heat flux increases in the region of the corner as  $y/H_f > 1$  whereas data from corner tests without a ceiling show a decline in the incident heat flux as  $y/H_f > 1$ .

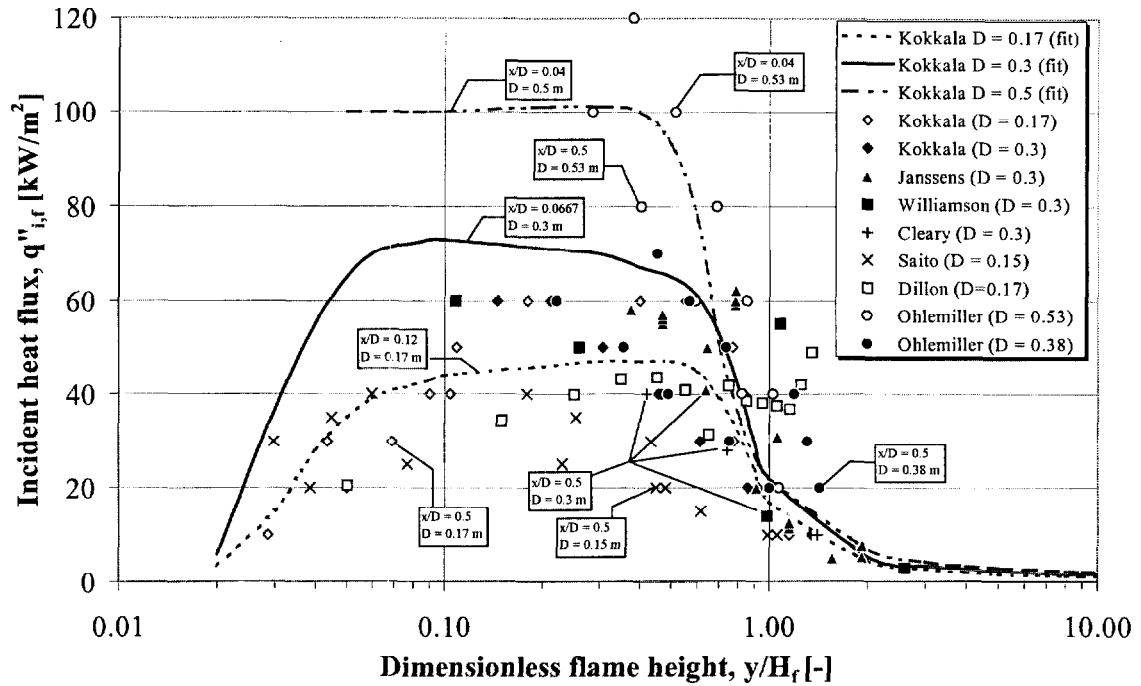


**Figure 10.** Heat flux from a burner flame as a function of dimensionless flame height.

Dillon analyzed the data provided by Kokkala in which it was found that the peak heat flux from a corner burner was simply a function of the width of the burner (Figure 11). Additional data by Saito [18] appears to match this relationship, however, Ohlemiller [20] obtained higher peak incident fluxes with the 0.53 m burner than what would be predicted by the relationship.

A "best-fit" power curve was obtained for the Kokkala data shown in Figure 11 such that

$$\dot{q}''_{i,f} = 171D^{0.75} \quad (11)$$

and this function was added to QFSM to obtain the incident heat flux from the burner flame to the wall. For the 0.17 m burner used in the ISO 9705 test, the function gives an incident flux of 45 kW/m<sup>2</sup>. This value is 25% less than the 60 kW/m<sup>2</sup> selected by Quintiere and used in the previous versions of QFSM. An incident heat flux of 45 kW/m<sup>2</sup> for the 100 kW burner output is in good agreement with the heat fluxes

measured by Dillon [17] and values by Janssens. However, this value is most likely too low for the 300 kW burner output.

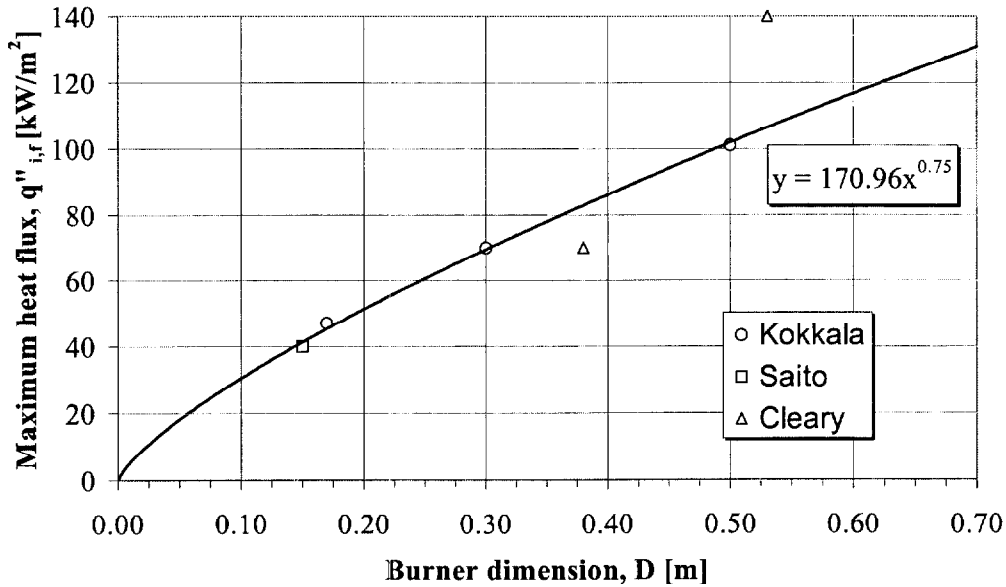


**Figure 11.** Maximum heat flux as a function of burner dimension.

For fires against vertical walls Beyler *et al.* [22] found that the heat flux to the wall appears to be a function of the energy release of the fire  $\dot{Q}$  and not the size of the base dimension  $D$ . It is not clear why the heat flux should be a function of  $D$  for a corner, as suggested by Kokkala, but a function of  $\dot{Q}$  for a wall. The radiative heat flux is given by

$$\dot{q}'' = \varepsilon \sigma T^4 \quad (12)$$

where

$$\varepsilon = 1 - e^{-\kappa l_m} \quad (13)$$

Seigel & Howel [23] approximate the mean beam length for an optically thin gas as

$$l_m = \frac{4V}{A} \quad (14)$$

For the case of a burner flame in a corner, the area and volume can be approximated to

$$A = H_f D \quad (15)$$

and

$$V = H_f D^2. \quad (16)$$

Hence

$$l_m = \frac{4H_f D^2}{H_f D} = 4D. \quad (17)$$

Thus according to this approximation, the incident flux is simply a function of  $D$ , as suggested by Kokkala. Further measurements and analysis may be required to support this conclusion and therefore no modifications were made to QFSM for vertical wall scenarios.

## 2.5 Flame spread heat flux

Hasemi *et al.* [24] performed experiments to measure the incident heat flux from a simulated burning surface using vertical gas burners in a corner arrangement with and without a ceiling. The measurements gave maximum incident heat fluxes of between 20 kW/m<sup>2</sup> and around 40 kW/m<sup>2</sup> for burner energy release rates of up to 60 kW.

Quintiere assumes a maximum heat flux for a spreading vertical flame of 30 kW/m<sup>2</sup> in his model. This value is comparable with Hasemi *et al.*'s data and thus no modifications to this parameter has been made in QFSM.

## 2.6 Summary of current QFSM relationships

### Flame height

i) when  $y_b < y_{f,ig}$

$H_f < H$  : use Hasemi continuous flame correlation.

$H_f > H$  : use Thomas/Karlsson flame extension correlation

such that  $H_f = H + L_f$

ii) when  $y_b \geq y_{f,ig}$  (burn-out)

use Quintiere's equation i.e. Equation (2)

### Initial pyrolysis height

Use flame height of burner at ignition as calculated above.

### Heat flux

Burning :  $\dot{q}_{i,f}''$  use Kokkala, (for  $D = 0.17$  m,  $\dot{q}_{i,f}'' = 45$  kW/m<sup>2</sup>)

Spread :  $\dot{q}_{i,f}'' = 30$  kW/m<sup>2</sup>

## **3. COMPARISON WITH PREVIOUS DATA**

### **3.1 Times to flashover**

The results from QFSM v1.4 were compared with previous results and experimental test data. Quintiere *et al.* [5] compared the previous version of QFSM with several series of ISO 9705 room/corner tests plus some additional tests conducted by the Federal Aviation Administration (FAA). Their study includes the necessary material property data and the time for the energy release from the fire to reach 1 MW (i.e. flashover). Where the comparison between the test data and prediction was poor Quintiere *et al.* modified the values of several of the material properties so as to improve the predicted to flashover compared with test data.

In this current study the results from Quintiere *et al.* were compared with QFSM v1.4 using only the unmodified reported material properties. Table 1 shows the experimental and calculated times to flashover. Examination of the predictions made by QFSM v1.4 against the previous version shows that in 11 cases the new version gives an improved prediction (Tests S1, S2, S3, S4, S8, S9, S10, S12, S13, E9 and E11).

In Tests S5 and S7 both versions of QFSM predicted flashover during the period in which the burner output was 100 kW whereas in the experiments flashover did not occur until the burner output was increased to 300 kW. Conversely in Test E7, both versions of QFSM did not predict flashover until the burner output was increased to 300 kW whereas flashover occurred much earlier in the experiment. In 2 cases (Tests

S12 and E11) the predicted times to flashover given by the two versions of QFSM straddle the test data with QFSM v1.3 giving shorter times and QFSM v1.4 longer times. In both cases, QFSM v1.4 is closer to the experimental values.

QFSM v1.4 also exhibited 5 cases (Tests S6, E2, E3, E6 and E10) in which the match between the predicted time to flashover was not as successful as QFSM v1.3. For Tests S6 and E10, QFSM v1.4 did not predict flashover whereas QFSM v1.3 and the experimental data gave times to flashover after the burner output was increased to 300 kW. In Test E2 the time to flashover predicted by QFSM v1.4 was longer than the experimental data and the prediction made by QFSM v1.3. However, flashover occurred during the 100 kW burner output phase of the test in both simulations and during the experiment. In Test E3 the time to flashover given by QFSM v1.4 was slightly quicker than that given by QFSM v1.3 and the experimental data but the difference is not significant since in all three cases flashover occurs soon after the burner output is increase to 300 kW.

Material		Test data	QFSM results using reported material properties	
			QFSM v1.3	QFSM v1.4
S1	Insulating Fiberboard	59	28	36
S2	Medium Density Fiberboard	131	76	96
S3	Particle Board	157	118	138
S4	Gypsum Board	∞	641	∞
S5	PVC Covered Gypsum Board	611	29	39
S6	Paper Covered Gypsum Board	640	613	∞
S7	Textile Covered Gypsum Board	639	38	68
S8	Textile Covered Mineral Wool	43	11	20
S9	Melamine Covered Particle Board	465	311	469
S10	Expanded Polystyrene (PS)	115	40	83
S11	Polyurethane Foam (rigid)	6	5	6
S12	Wood Panel (spruce)	131	108	144
S13	Paper Covered Particle Board	143	216	170
E1	Painted Gypsum Paper Plaster Board	∞	∞	∞
E2	Ordinary Birch Wood	160	263	445
E3	Textile Covering on Gypsum Board	670	623	602
E4	Melamine Faced High Density Non-combustible Board	∞	638	610
E5	Plastic Faced Steel Sheet on Mineral Wool	∞	∞	∞
E6	FR Particle Board Type B1	630	∞	111
E7	Combustible Faced Mineral Wool	75	601	646
E8	FR Particle Board	∞	∞	∞
E9	Plastic Faced Steel Sheet on Polyurethane Foam	215	362	338
E10	PVC Wallcarpet on Gypsum Board	650	613	∞
E11	Extruded Polystyrene Foam	80	47	91

**Table 1.** Comparison times to flashover from experimental test data and QFSM predictions using properties given by Quintiere *et al.* [5].

It is interesting to note that for Test E6 by increasing the heat of gasification from the reported value of 1.4 kJ/g to 1.6 kJ/g, QFSM v1.4 predicts flashover does not occur. A further increase to 1.8 kJ/g gives a predicted time to flashover of 601 s. The predicted energy release rates for these heat of gasification values are shown in Figure 12. Clearly in this case, the prediction of energy release and thus time to flashover is very sensitive to the heat of gasification.

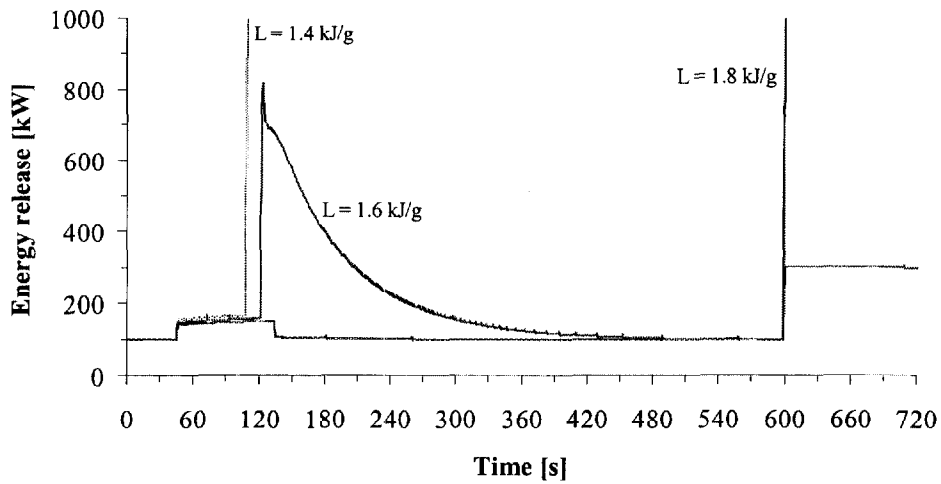


**Figure 12.** Sensitivity of predicted energy release rate by QFSM v1.4 for Test E6, FR Particle Board Type B1.

For Test E7, both versions of QFSM fail to predict the rapid fire growth obtained in the test and onset of flashover after 75 s. However, comparing the predicted energy release (Figure 13) it can be seen that QFSM v1.4 comes closer to reaching flashover at around 43 s but the energy release only reaches a peak of 435 kW before decaying again. As with Test E6, a slight adjustment to the material properties may lead to a more successful prediction of flashover.

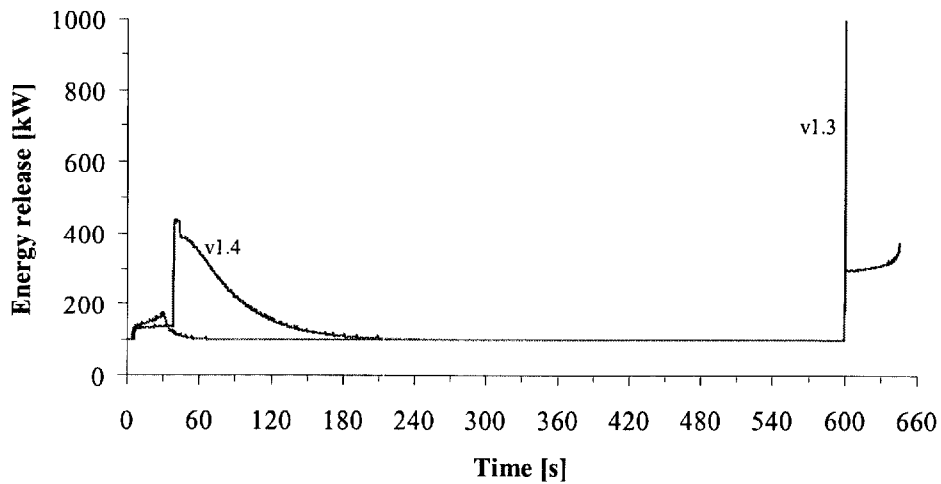


**Figure 13.** Comparison of the predicted energy release rate by QFSM for Test E7, Combustible Faced Mineral Wool.

In addition Quintiere, Torero, Long, Dillon, Wu & Heater [25] report material properties and experimental times to flashover in the ISO 9705 room/corner tests taken from a study conducted at BRI, Japan. These data were used to compare the predictions of the two versions of QFSM as shown in Table 2. In general, the time to flashover predictions given by QFSM v1.4 do not differ significantly from those given by QFSM v1.3. For Test J7-Q, QFSM v1.4 gives a somewhat longer time to flashover in comparison with the experiment and QFSM v1.3. In Test J8-L both versions of QFSM fail to predict the longer time to flashover after the burner is increased to its 300 kW output but instead give times to flashover during the 100 kW burner phase of the simulation.

Material		Test data	QFSM results using reported material properties	
			QFSM v1.3	QFSM v1.4
J7-Ao	PVC Wall Paper (300 g/m <sup>2</sup> ) on Gypsum Board	610	605	601
J7-Q	Soft Fiberboard	54	41	102
J8-B	Rayon Wall Paper (300 g/m <sup>2</sup> ) on Gypsum Board	672	627	604
J8-C	Emulsion Paint on Gypsum Board	∞	644	638
J8-D	Acrylic Paint on Gypsum Board	∞	633	608
J8-E	Surface Treatment on Gypsum Board	∞	649	612
J8-F	FR Surface Treatment on Gypsum Board	∞	654	612
J8-H	FR Polyethylene Foam on Metal Plate	∞	683	622
J8-L	PVC Wall Paper (800 g/m <sup>2</sup> ) on Gypsum Board	834	63	79

**Table 2.** Comparison times to flashover from experimental test data and QFSM predictions using properties given by Quintiere *et al.* [25].

Figure 14 and Figure 15 show comparisons between the experimental data and the predicted times to flashover from QFSM v1.3 and v1.4 respectively for the Swedish, Japanese and Eurefic data.

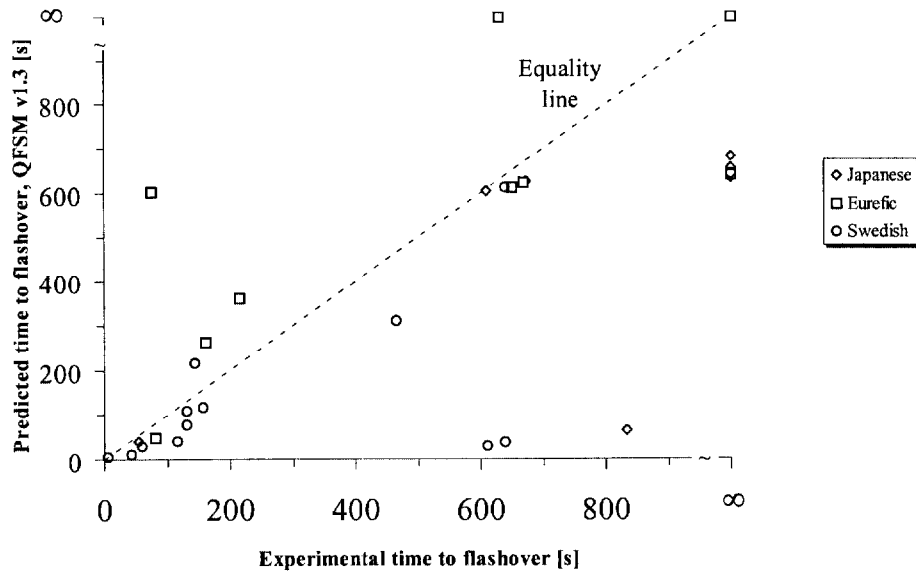


**Figure 14.** Comparison between the experimental data and the predicted times to flashover from QFSM v1.3.

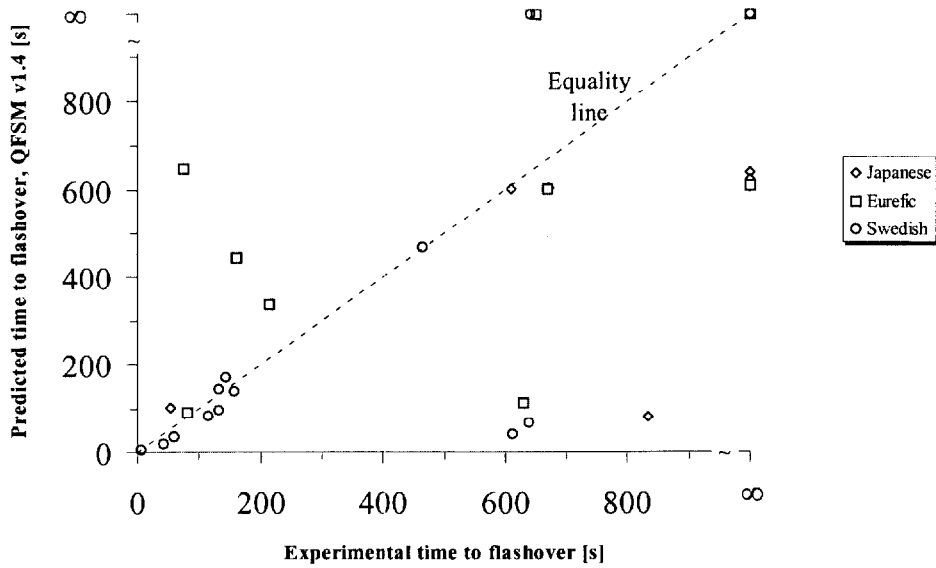


**Figure 15.** Comparison between the experimental data and the predicted times to flashover from QFSM v1.4.

### 3.2 Performance ranking

Quintiere *et al.* [5] also compared the results from a series of tests conducted by the FAA investigating the performance of aircraft interior linings. These results are compared with the two versions of QFSM as shown in Table 3.

Material		Test data	QFSM results using reported material properties	
			QFSM v1.3	QFSM v1.4
F1	Epoxy Fiberglass Faced Nomex 1/4 in. Honeycomb Core	70	49	78
F2	Phenolic Fiberglass Faced Nomex 1/4 in. Honeycomb Core	230	606	269
F3	Epoxy Kevlar Faced Nomex 1/4 in. Honeycomb Core	-	80	147
F4	Phenolic Kevlar Faced Nomex 1/4 in. Honeycomb Core	70	49	86
F5	Phenolic Graphite Faced Nomex 1/4 in. Honeycomb Core	190	∞	∞
F6	ABS with 20% PVC 1/16 in. Sheet	-	73	104
F7	Polycarbonate 1/16 in. Sheet	-	118	243
F8	ULTEM 1/16 in. Sheet	-	696	623

**Table 3.** Comparison times to flashover from full-scale test results and QFSM predictions for FAA data.

QFSM v1.4 obtains the same time-to-flashover order as QFSM v1.3 for the 4 materials in which the experiments achieved flashover. In Test F2, QFSM v1.4 obtains a much better match with the experimental data compared with the prediction made by QFSM v1.3. In Tests F1 and F4, QFSM v1.4 also improves on the prediction compared with QFSM v1.3.

### 3.3 Energy release

Dillon [17] conducted and analyzed a number of ISO 9705 room/corner tests at the LSF laboratory in Italy using several materials. Dillon reports the properties for each material and used those data to make predictions for the energy release rate using QFSM v1.3. The predicted energy release rate was compared with the measured test data and where the two did not match Dillon varied the properties until an improved match was obtained. In the current study, the measured energy release data are compared with predictions from the two versions of QFSM using the unmodified material properties reported by Dillon.

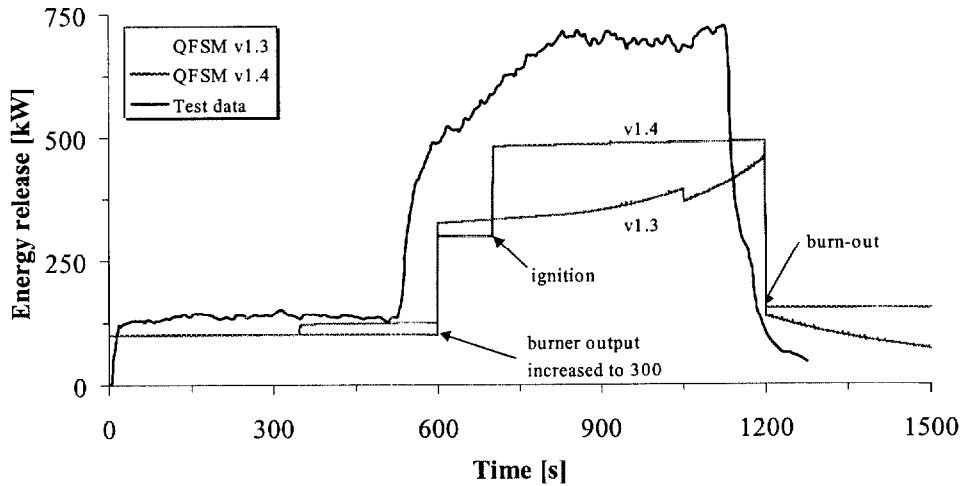


**Figure 16.** Comparison between measured and predicted energy release, LSF Test R 4.01, Fire retarded chipboard.

Figure 16 shows the measured and predicted energy release rate for Test R 4.01, Fire retarded chipboard. QFSM v1.4 obtains a closer prediction than QFSM v1.3 partly

because ignition does not occur until after the burner output is increased to 300 kW whereas QFSM v1.3 predicts that ignition occurs at around 350 s.

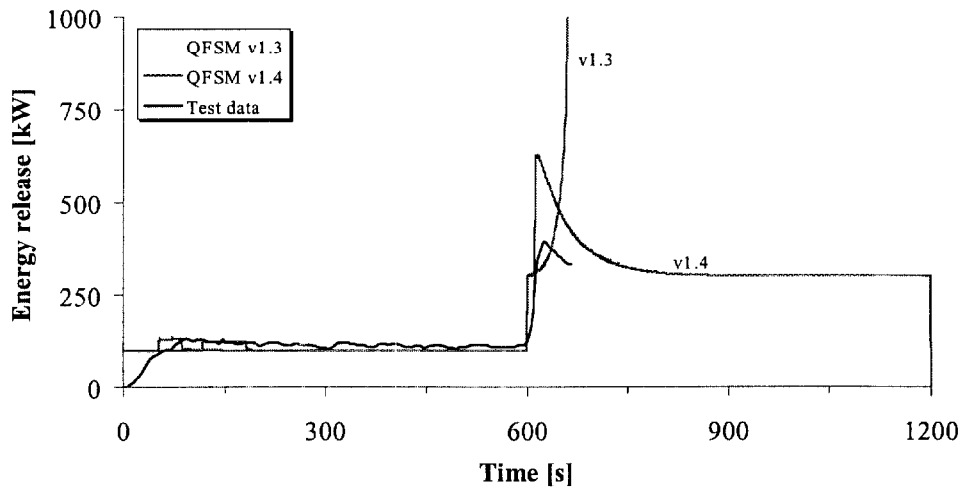


**Figure 17.** Comparison between measured and predicted energy release, LSF Test R 4.02, Paper faced gypsum board.

For Test R 4.02, Paper faced gypsum board, QFSM v1.3 predicts flashover conditions in the room when the burner output is increased to 300 kW. The measured energy release rate and the prediction from QFSM v1.4 both show an increase in the energy release rate at this point but the room does not reach flashover conditions (Figure 17).

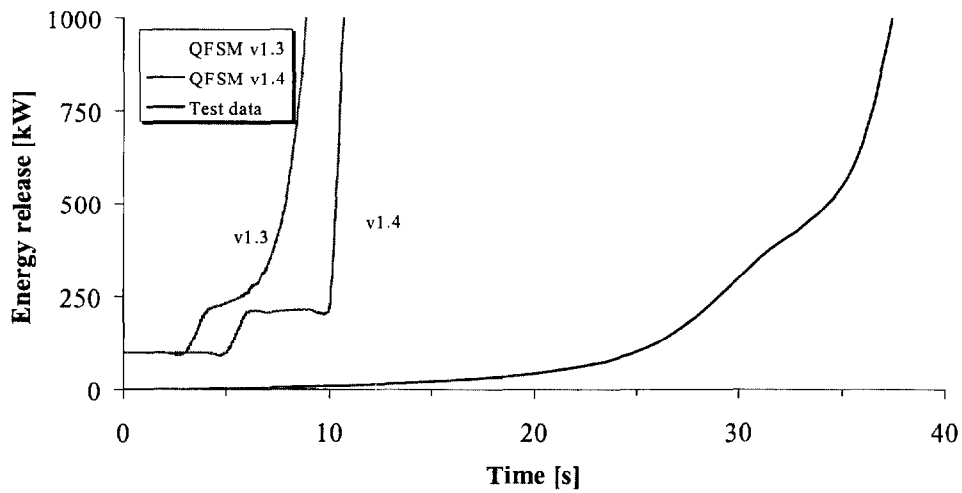


**Figure 18.** Comparison between measured and predicted energy release, LSF Test R 4.04, Polyurethane panel with paper facing.

In Test R 4.04, Polyurethane panel with paper facing, the test measurements show a rapid increase in the energy release rate (Figure 18) with flashover occurring just before 40 seconds. The two versions of QFSM both predict rapid fire growths with flashover being attained at around 7 and 10 seconds for QFSM v1.3 and v1.4 respectively. Since in the configuration of the ISO 9705 test the exhaust hood is located outside of the room, a delay is introduced between the actual energy release at the burner and measured energy release in the exhaust hood. Were this delay accounted for in the comparison between the measurements and predictions, it might be expected that a closer match would be obtained.

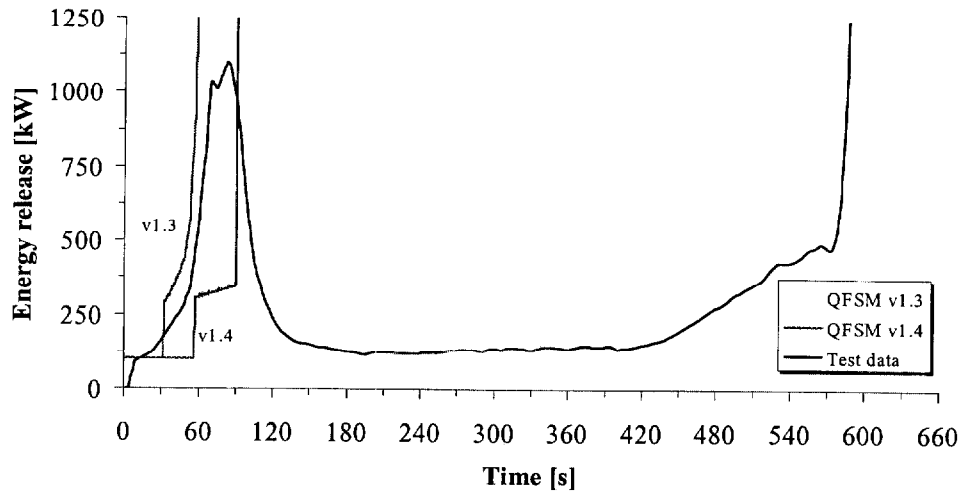


**Figure 19.** Comparison between measured and predicted energy release, LSF  
Test R 4.05, Extruded polystyrene board.

The measured energy release for Test R 4.05, Extruded polystyrene board, shows a peak at around 90 seconds followed by a decay until just before the burner output is increased to 300 kW where flashover occurs (Figure 19). The two versions of QFSM both predict flashover at the earlier stage of the test with QFSM v1.3 following the test data more closely than QFSM v1.4.

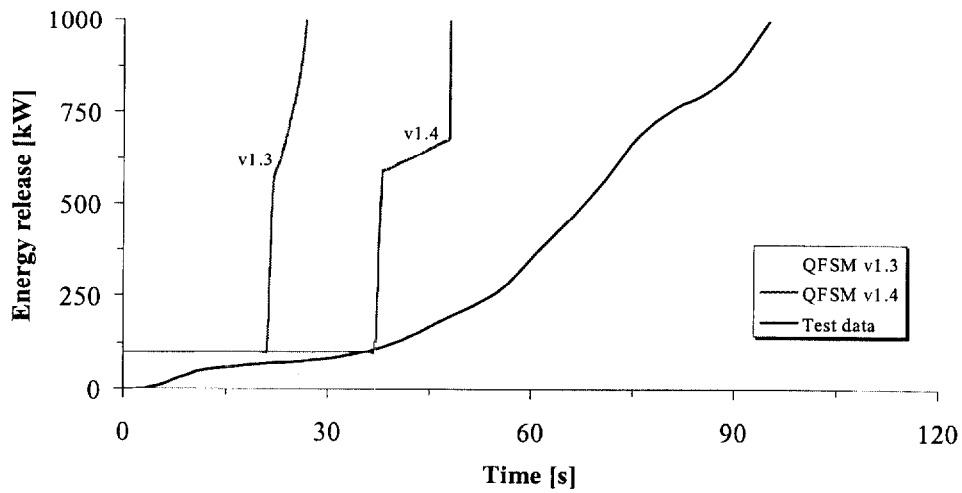


**Figure 20.** Comparison between measured and predicted energy release, LSF Test R 4.06, Acrylic glazing.

The test results and predictions for R 4.06, Acrylic glazing show similar trends with all three rapidly reaching flashover (Figure 20). The delay in the measurement (as discussed above) may also be relevant to this test.

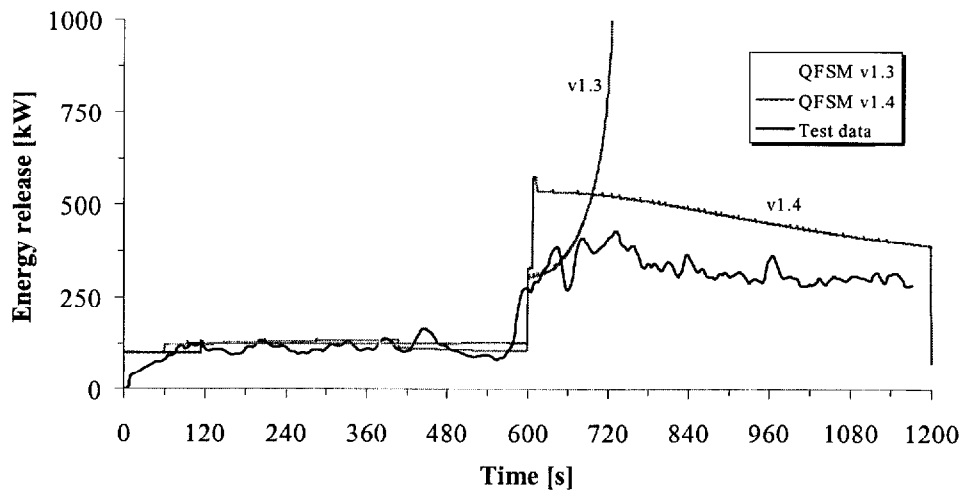


**Figure 21.** Comparison between measured and predicted energy release, LSF Test R 4.07, Fire retarded PVC.

For Test R 4.07, Fire retarded PVC, the prediction for energy release by QFSM v1.4 matches the experimental data significantly better than QFSM v1.3 (Figure 21). Whereas QFSM v1.3 predicts that flashover will occur when the burner output is increased to 300 kW, QFSM v1.4 exhibits the increased energy release at this point but also predicts the gradual decay thereafter.

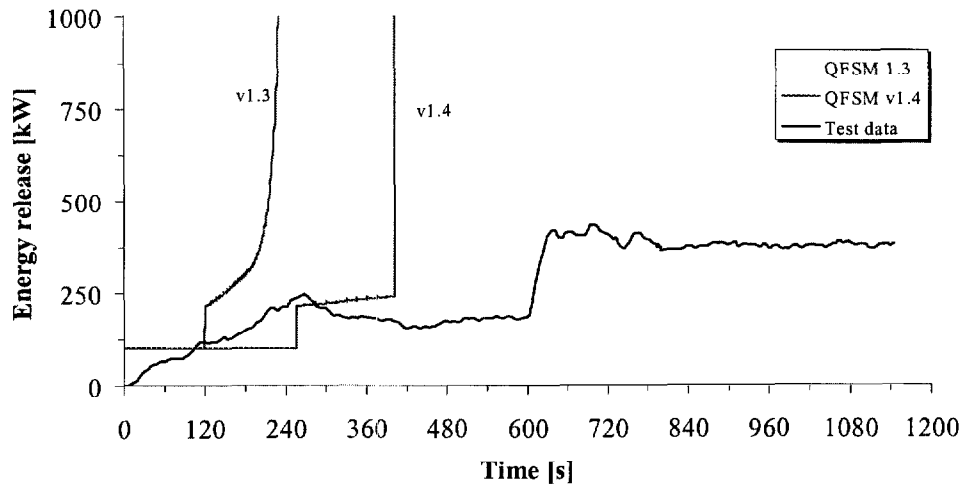


**Figure 22.** Comparison between measured and predicted energy release, LSF Test R 4.08, 3-layered fire retarded polycarbonate panel.

For Test R 4.08, 3-layered fire retarded polycarbonate panel, QFSM v1.4 makes a slightly better prediction of the energy release (Figure 22) but both version of the model predict the onset of flashover during the 100 kW burner output phase whereas the experimental data does not show this.

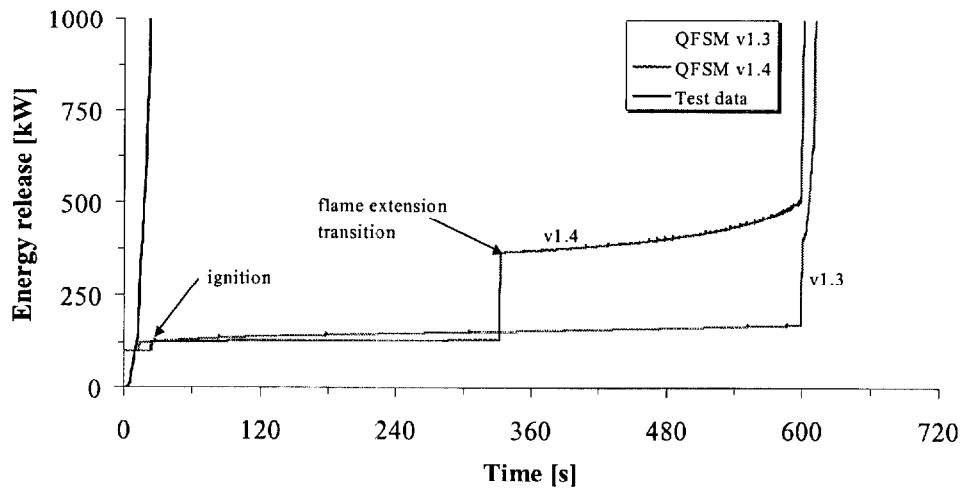


**Figure 23.** Comparison between measured and predicted energy release, LSF  
Test R 4.09, Varnished massive timber.

Both versions of QFSM fail to predicted the experimentally measured energy release for Test R 4.09, Varnished massive timber (Figure 23). The behaviour of QFSM v1.4 is somewhat different to QFSM v1.3 in this case. QFSM v1.4 exhibits a jump in its predicted energy release at around 340 s and then a slow growth until the burner output is increased to 300 kW. The jump at around 340 s is due to the flame length transition from a vertical corner flame to a flame extending under a ceiling as described in §2.2.

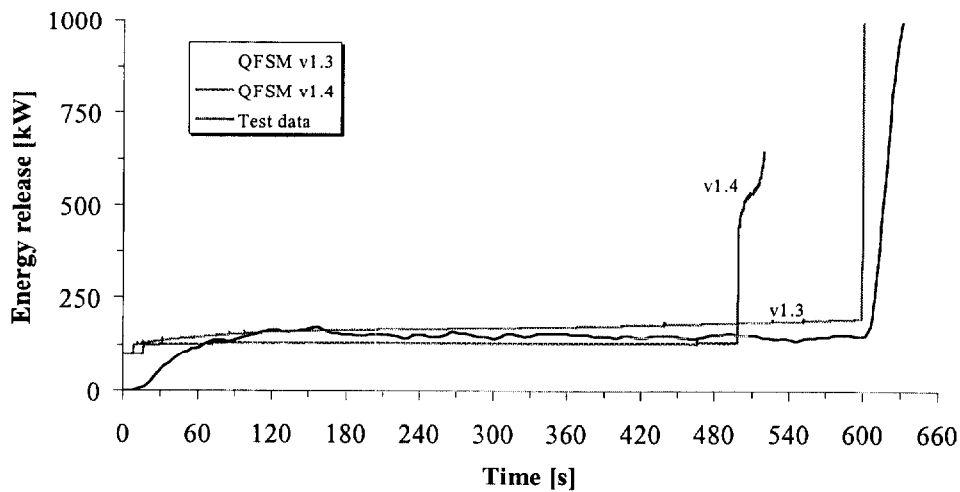


**Figure 24.** Comparison between measured and predicted energy release, LSF Test R 4.10, Fire retarded plywood.

For Test R 4.10, Fire retarded plywood QFSM v1.3 shows a similar prediction to the experimental data (Figure 24). However, QFSM v1.4 predicts that flashover would occur before the burner output was increased to 300 kW.

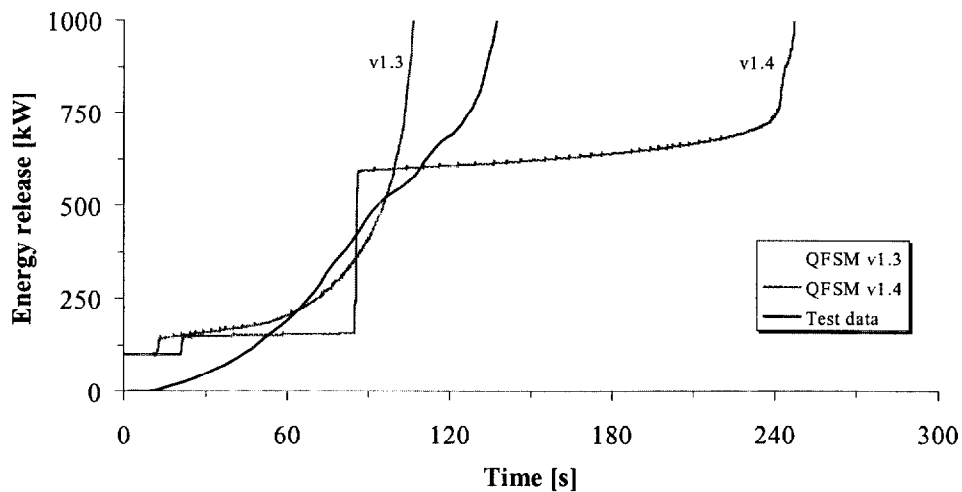


**Figure 25.** Comparison between measured and predicted energy release, LSF Test R 4.11, Normal plywood.

For Test R 4.11, Normal plywood, the predictions for the energy release by the two versions of QFSM straddle the measured data (Figure 25) with QFSM v1.3 making a generally better prediction than QFSM v1.4.

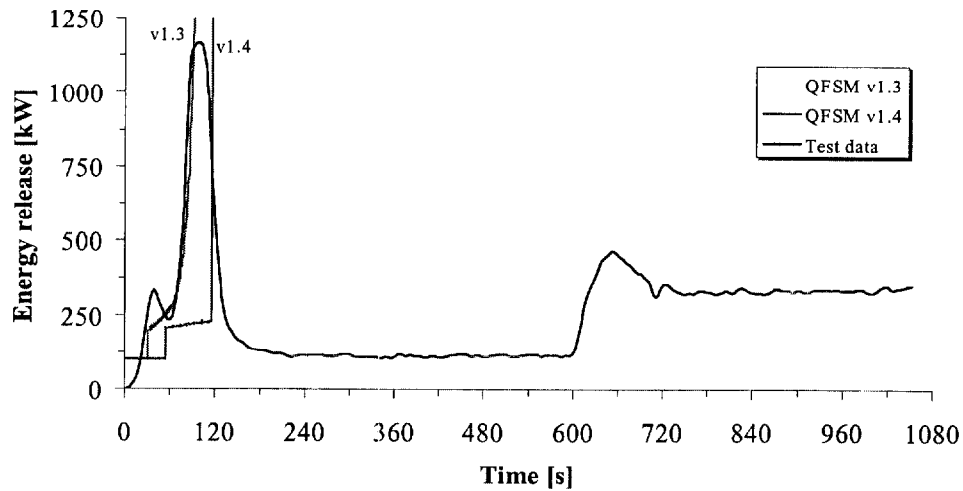


**Figure 26.** Comparison between measured and predicted energy release, LSF  
Test R 4.20, Fire retarded expanded polystyrene board (40 mm).

The predicted energy release from QFSM v1.3 is slightly better than that made by QFSM v1.4 at least for the initial rapid growth in the fire (Figure 26) for Test R 4.20, Fire retarded expanded polystyrene board (40 mm). Both versions of the model are unable to simulate the ignition of the remaining material when the burner output is increased to 300 kW.

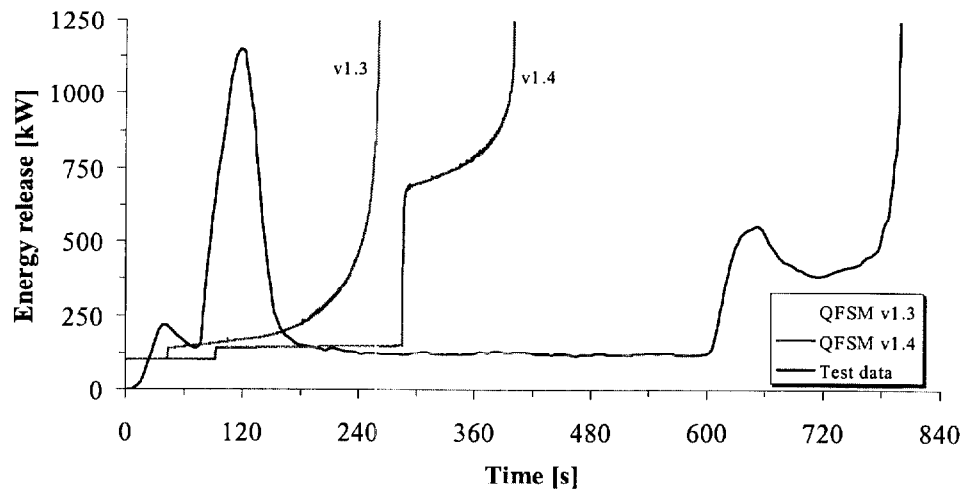


**Figure 27.** Comparison between measured and predicted energy release, LSF Test R 4.21, Fire retarded expanded polystyrene board (80 mm).

Figure 27 shows the measured energy release curve and predictions for Test R 4.21, Fire retarded expanded polystyrene board (80 mm). Both versions of QFSM give predictions somewhere between the experimental data. If the time to 1 MW for flashover criteria was selected then QFSM would have predicted times to flashover during the 100 kW burner output phase but with times two or three times as long. Dillon [17] reports that the behaviour of this material made predictions difficult and this is confirmed in this study too.

In summary, for the LSF tests QFSM v1.4 makes significant improvements over the predictions for energy release made by QFSM v1.3 in 2 cases (Tests R 4.05 and R 4.07). In an additional 2 cases (Tests R 4.04 and R 4.06) QFSM v1.4 makes a slight improvement in the prediction. In 3 cases (Tests R 4.05, R 4.11 and R 4.20) the QFSM v1.4 predictions are not as good as for QFSM v1.3 but the differences are not generally significant. Only in Test R 4.10 does QFSM v1.4 predict an energy release curve that is significantly worse than that given by QFSM v1.3.

#### 4. USER INTERFACE

A new user-friendly front-end interface has been developed for the QFSM program. The interface was written in Microsoft Visual Basic version 5.0 to run under a Windows 95/98 environment. The interface can be used to read in existing model input files, create new input files, execute the main QFSM program and create simple on screen plots of the results. The front-end also includes an online help file that describes the various input parameters [26].

The original QFSM program has been retained as a stand-alone executable compiled from the FORTRAN source code. Some minor additions have been made to the FORTRAN code to allow the front-end to execute the code. However, the front-end is not required to use the QFSM program and the model can be executed solely from the DOS environment.

The complete package consisting of the main QFSM program, the interface application and associated system files, the online help documentation and additional support files are available as a single self-extracting distribution file. This simplifies dissemination of the package if the intention is to make it available from a web site or such like.

The distribution file should be copied to a temporary folder on the users local disk drive. Once the files have been extracted into the temporary folder the user is able to install the QFSM program and interface into a folder of their own choosing. The files in the temporary folder can then be deleted.

The interface consists of the data input window and the analysis window. The data input window (Figure 28) allows the user to input and edit the various parameters required by QFSM. The parameters have been categorized into four groups; General, Fire source, Lining material and Compartment. Each group can be accessed by clicking on the appropriate tab. There is also a tab that allows the user to set various options for QFSM and the interface. To perform a simulation, the user clicks on the Execute... button and

the interface will run the QFSM model. A simple DOS text window that displays the simulation's progress will appear while QFSM is running.

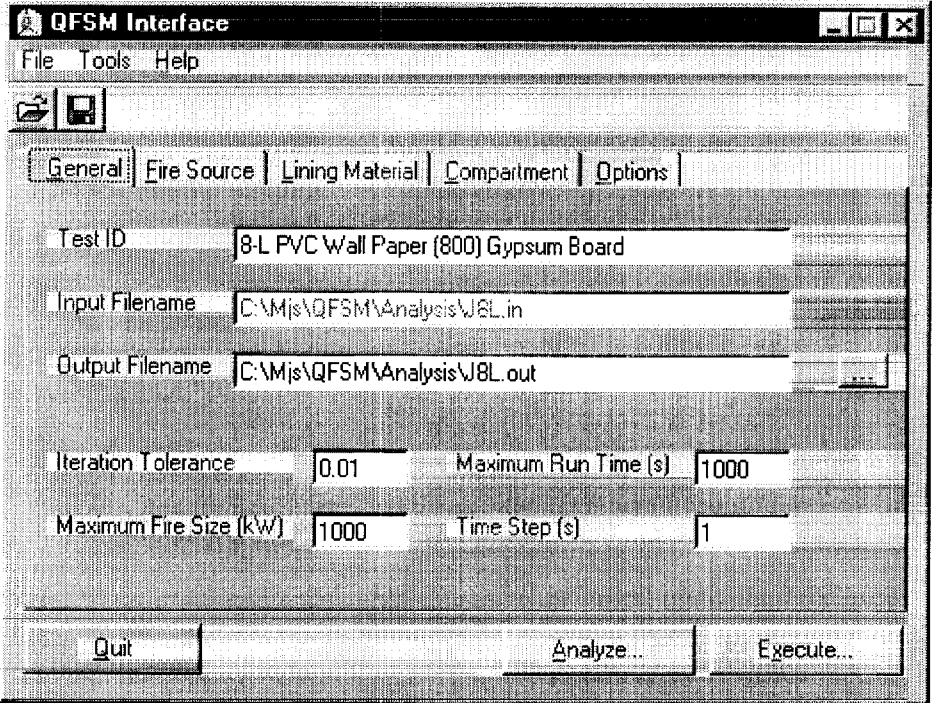


**Figure 28.** The QFSM interface data input window.

Once the simulation is complete the DOS window will be automatically closed and the user is then able to plot the results on the screen by clicking on the Analyze... button. This will display the analysis window (Figure 29) in which graphs of various calculated parameters can be viewed.

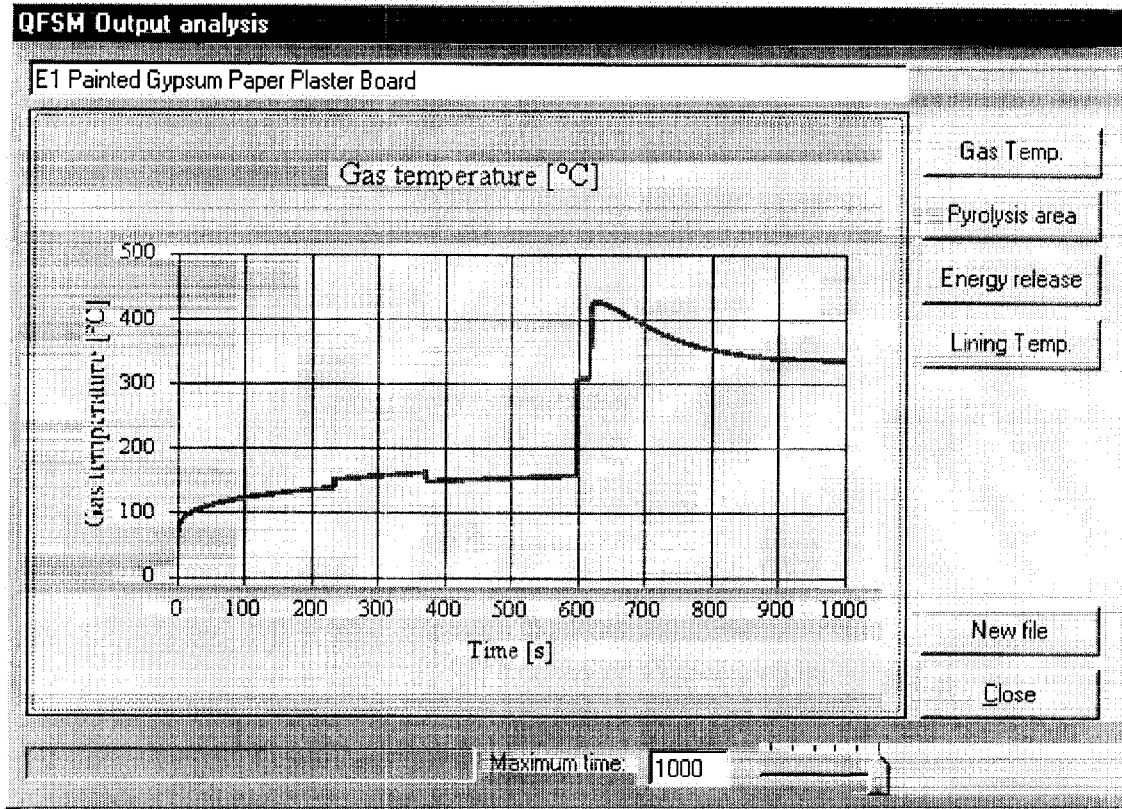


**Figure 29.** The QFSM interface output analysis window.

The user can click on the various buttons on the right-hand side of the window to view the calculated results. The maximum simulation time is shown in the text window at the bottom of the screen and the user can use the slider next to it to change the maximum value for the time scale.

## 5. CONCLUSIONS

Several of the assumptions and simplifications necessary during the initial development of QFSM have been investigated and revised on the basis of new experimental and theoretical studies obtained from the literature. The height of the ignition source flames and their heat flux to the wall surface have been modified. The extension of flames under a ceiling have also been included in the revisions.

Comparing the predictions from QFSM v1.4 with QFSM v1.3 and a range of experimental data shows that QFSM v1.4 in general gives an improved match with times to flashover and the predicted energy release obtained in the experiments. However, QFSM v1.4 may fail to predict flashover for the 100 kW burner output when compared to some experimental results. Instead, flashover does not occur until the burner output is increased to 600 kW.

A user-friendly interface for QFSM has been implemented in a Windows environment. The interface enhances the setting up, execution and preliminary analysis of QFSM runs. However, the core QFSM program can still be used without the necessity of the interface. An integrated set of help documentation is included. The complete package can be distributed as a single self-extracting program that simplifies its installation.

## **6. REFERENCES**

1. Quintiere J. G., A simulation model for fire growth on materials subject to a room-corner test. *Fire Safety Journal* 20 (1993) pp.313-339.
2. Quintiere, J. G., Estimating fire growth on compartment interior finish materials, Department of Fire Protection Engineering, University of Maryland, College Park, MD, 1995.
3. Haynes, G. A., Analysis of a model to predict flame spread over a PMMA wall in a compartment, M.S. Thesis, Department of Fire Protection Engineering, University of Maryland, College Park, Maryland, 1996.
4. Janssens, M., Predictions of ISO 9705 room/corner test using a simple model, Interscience Communications Limited, Fire and Materials, Proceedings of the 4<sup>th</sup> International Conference and Exhibition, 1995, pp.73-83.

5. Quintiere J. G., Haynes G. & Rhodes B. T. Applications of a model to predict flame spread over interior finish materials in a compartment. *Journal of Fire Protection Engineering*. 7 (1) 1995 pp.1-13.
6. Dillon S. E. QFSM code modifications, Private communication, Nov 1997.
7. ISO 9705, International Standard, Fire tests—full scale room test for surface products, First Edition, Reference Number ISO/TC92/WG7/N124, 1993-05-15.
8. Kokkala, M. A., Characteristics of a flame in an open corner of walls, Interflam '93, Inter Science Communications Limited, London, England, 1993, pp.13-24.
9. Kokkala, M., Ulf Göransson, Johan Söderbom, Five large-scale room fire experiments: Project 3 of the EUREFIC fire research programme, Technical Research Centre of Finland, Espoo, 1992.
10. Zukoski, E. E., Fluid dynamic aspects of room fires, Proceedings of the First International Symposium on Fire Safety Science, ed. C. E. Grant and P. J. Pagni, Hemisphere Publishing Corp., NY, 1986, pp. 1-30.
11. Gross, D. Measurements of flame lengths under ceilings, NISTIR 88-3835, National Institute of Standards and Technology, Gaithersburg, MD, 1988.
12. Hasemi, Y. Experimental wall flame heat transfer correlations for the analysis of upward wall flame spread, *Fire Science and Technology*, Vol. 4, No. 2, 1994, pp.75-90.
13. Thomas P. H., & Karlsson B., On the length of flames under ceilings. Department of Fire Safety Engineering, Lund University, SE-LUTVDG/TVBB-3059, December 1990.

14. Babrauskas V., Flame length under ceilings. *Fire and Materials* Vol.4 No.3 1980 pp.119-126.
15. Andersson C. & Giacomelli C., Ett modellrum i lågor, Dept. of Fire Safety Engineering, Lund University, 1985.
16. You H. Z. & Faeth G. M., An investigation of fire impingement on a horizontal ceiling, Mechanical Engineering Dept., Pennsylvania State University, 1981.
17. Dillon S. E., Analysis of the ISO 9705 room/corner test: Simulations, correlations and heat flux measurements. NIST-GCR-98-756, National Institute of Standards and Technology, Gaithersburg, MD, August 1998.
18. Saito K., Study of fire induced flow along the vertical corner wall. Part 2. NIST-GCR-98-756, National Institute of Standards and Technology, Gaithersburg, MD, April 1993.
19. Ohlemiller T. J., Cleary T. G. & Shields J. R., Effect of ignition conditions on upward flame spread on a composite material in a corner configuration. Materials and Process Challenges: Aging Systems, Affordability, Alternative Applications. SAMPE Symposium and Exhibition, 41st International Proceedings. Volume 41, Book 1. Society for the Advancement of Material and Process Engineering (SAMPE). March 24-28, 1996, Anaheim, CA.
20. Ohlemiller T. J. & Shields J. R., The effect of surface coatings on fire growth over composite materials in a corner configuration. *Fire Safety Journal* 32 (1999) 173-193.
21. Quintiere J. G. & Cleary T. G. Heat flux from flames to vertical surfaces, *Fire and Technology*, Second Quarter, 1994, pp. 209 - 231.

22. Back G., Beyler C., DiNenno P., & Tatem P., Wall incident heat flux distributions resulting from an adjacent fire. International Association for Fire Safety Science. Proceedings 4<sup>th</sup> International Symposium, July 13-17 1994, Ontario, Canada.
23. Seigel R. & Howell J. R., Thermal radiation heat transfer, Second Edition. McGraw-Hill Book Company, New York, 1981.
24. Hasemi Y., Yoshida M., Takashima S., Kikuchi R. & Yokobayashi Y. Flame length and flame heat transfer correlations in corner-wall and corner-wall-ceiling configurations, Interflam '96. Inter Science Communications Limited, London, England, 1996, pp.179-188.
25. Quintiere J. G., Torero J. L., Long R. T., Dillon S. E., Wu N. & Heater D. Material fire properties. International Fire and Cabin Safety Research Conference held on November 16-20, 1998, Atlantic City, NJ.
26. Spearpoint M. J. QFSM Interface documentation, University of Maryland, Sept 1999.

NIST-114 (REV. 6-93) ADMAN 4.09 <b>U.S. DEPARTMENT OF COMMERCE</b> NATIONAL INSTITUTE OF STANDARDS AND TECHNOLOGY <b>MANUSCRIPT REVIEW AND APPROVAL</b>		(ERB USE ONLY)	
		ERB CONTROL NUMBER <b>G</b>	DIVISION
		PUBLICATIONS REPORT NUMBER <b>No. NIST-CCR 99-782</b>	CATEGORY CODE
INSTRUCTIONS: ATTACH ORIGINAL OF THIS FORM TO ONE (1) COPY OF MANUSCRIPT AND SEND TO: WERB SECRETARY, BUILDING 820, ROOM 125		PUBLICATION DATE <b>November 1999</b>	NO. PRINTED PAGES
TITLE AND SUBTITLE (CITE IN FULL) <b>Flame Spread Model Progress: Enhancements and User Interface</b>			
CONTRACT OR GRANT NUMBER <b>60NANB6D0120</b>		TYPE OF REPORT AND/OR PERIOD COVERED <b>October 1999</b>	
AUTHOR(S) (LAST NAME, FIRST INITIAL, SECOND INITIAL) <b>Spearpoint, M.J. and Dillon, S.E.</b>		PERFORMING ORGANIZATION (CHECK (X) ONE BOX) <input type="checkbox"/> NIST/GAITHERSBURG <input type="checkbox"/> NIST/BOULDER <input type="checkbox"/> NIST/JILA	
LABORATORY AND DIVISION NAMES (FIRST NIST AUTHOR ONLY)			
SPONSORING ORGANIZATION NAME AND COMPLETE ADDRESS (STREET, CITY, STATE, ZIP) <b>U.S. Department of Commerce, National Institute of Standards and Technology, Gaithersburg, MD 20899</b>			
PROPOSED FOR NIST PUBLICATION			
<input type="checkbox"/>	JOURNAL OF RESEARCH (NIST JRES)	<input type="checkbox"/>	MONOGRAPH (NIST MN)
<input type="checkbox"/>	J. PHYS. & CHEM. REF. DATA (JPCRD)	<input type="checkbox"/>	NATL. STD. REF. DATA SERIES (NIST NSRDS)
<input type="checkbox"/>	HANDBOOK (NIST HB)	<input type="checkbox"/>	FEDERAL INFO. PROCESS. STDS. (NIST FIPS)
<input type="checkbox"/>	SPECIAL PUBLICATION (NIST SP)	<input type="checkbox"/>	LIST OF PUBLICATIONS (NIST LP)
<input type="checkbox"/>	TECHNICAL NOTE (TN)	<input type="checkbox"/>	INTERAGENCY/INTERNAL REPORT (NISTIR)
<input type="checkbox"/>		<input checked="" type="checkbox"/>	LETTER CIRCULAR
			BUILDING SCI. SERIES
			PRODUCT STANDARDS
			OTHER
			NIST-GCR-
PROPOSED FOR NON-NIST PUBLICATION (CITE FULLY): <input type="checkbox"/> -U.S.			
PUBLISHING MEDIUM: <input type="checkbox"/> PAPER <input type="checkbox"/> DISKETTE <input type="checkbox"/> CD-ROM <input type="checkbox"/> WWW <input type="checkbox"/> OTHER			
SUPPLEMENTARY NOTES			
ABSTRACT (A 2000-CHARACTER OR LESS FACTUAL SUMMARY OF MOST SIGNIFICANT INFORMATION. IF DOCUMENT INCLUDES A SIGNIFICANT BIBLIOGRAPHY OR LITERATURE SURVEY, CITE IT HERE. SPELL OUT ACRONYMS ON FIRST REFERENCE.) (CONTINUE ON SEPARATE PAGE, IF NECESSARY.) <b>This report describes the enhancements made to Quintiere's flame spread model based on worked published in the literature by other researchers. The height of the ignition source flame, its extension under a horizontal ceiling and the incident heat flux to a target material have been addressed.</b>  <b>The results from the enhanced version of the model have been compared with those obtained from an earlier version of the model and with experimental data. The new version generally shows an improvement over the previous versions although there are isolated instances in which this is not the case.</b>  <b>The report also briefly describes a user-friendly Windows based front-end that has been developed for the enhanced version of the model. The interface can be used to read in existing model input files, create new input files, execute the main QFSM program and create simple on screen plots of the results. The front-end also includes an online help file that describes the various input parameters. A single self-extracting file containing the QFSM model, the interface, the help documentation and associated support files has been created to simplify distribution and installation of the software.</b>			
KEY WORDS (MAXIMUM OF 9; 28 CHARACTERS AND SPACES EACH; SEPARATE WITH SEMICOLONS; ALPHABETIC ORDER; CAPITALIZE ONLY PROPER NAMES) computer models; corner tests; fire growth; flame height; flame resistant materials; flame spread; gypsum board; heat flux; wood			
AVAILABILITY: <input checked="" type="checkbox"/> UNLIMITED <input type="checkbox"/> FOR OFFICIAL DISTRIBUTION - DO NOT RELEASE TO NTIS <input type="checkbox"/> ORDER FROM SUPERINTENDENT OF DOCUMENTS, U.S. GPO, WASHINGTON, DC 20402 <input checked="" type="checkbox"/> ORDER FROM NTIS, SPRINGFIELD, VA 22161		NOTE TO AUTHOR(S): IF YOU DO NOT WISH THIS MANUSCRIPT ANNOUNCED BEFORE PUBLICATION, PLEASE CHECK HERE. <input type="checkbox"/>	